Oxytocin analogues for the oral treatment of abdominal pain

Thomas Kremsmayr,[1] Gudrun Schober,[2] Matthias Kaltenböck,[1] Bradley L. Hoare,[1] Stuart M. Brierley[2,3] and Markus Muttenthaler[1,4]*

[1] University of Vienna, Faculty of Chemistry, Institute of Biological Chemistry, Währinger Straße 38, 1090 Vienna, Austria

[2] Visceral Pain Research Group, Hopwood Centre for Neurobiology, Lifelong Health Theme, South Australian Health and Medical Research Institute (SAHMRI), North Terrace, Adelaide, South Australia 5000, Australia

[3] Faculty of Health and Medical Sciences, University of Adelaide, North Terrace, Adelaide, South Australia 5000, Australia

[4] Institute for Molecular Bioscience, The University of Queensland, 4072 Brisbane, Queensland, Australia

KEYWORDS: oxytocin, gastrointestinal disorders, abdominal pain, peptide drug development, oral peptide therapeutics

ABSTRACT

Abdominal pain presents an onerous day-to-day reality for millions of people affected by chronic gastrointestinal disorders such as irritable bowel syndrome (IBS) and inflammatory bowel diseases (IBD). The oxytocin receptor (OTR) has emerged as a potential novel analgesic drug target as OTR expression is upregulated on colon-innervating nociceptors, which are accessible *via* luminal delivery in chronic visceral hypersensitivity states. However, the low gastrointestinal stability of the endogenous OTR peptide ligand oxytocin (OT) is a crucial bottleneck for therapeutic development. Here, we report the rational development of the first series of fully gut-stable and potent OT analogues, laying the foundation for a new area of oral and gut-specific peptide therapeutics. Compound optimisation guided by systematic structure-gut-stability-activity relationship analysis yielded highly stable analogues ($t_{1/2}$ >24 h, compared to $t_{1/2}$ <10 min of OT in intestinal fluid) equipotent to native OT (~3 nM) and with enhanced selectivity for OTR. Colon-targeted local luminal administration of the lead compound significantly reduced colonic mechanical hypersensitivity in a concentration-dependent manner in an *in vivo* mouse model of chronic abdominal pain. Moreover, oral administration of the lead compound also significantly reduced colonic mechanical hypersensitivity in this abdominal pain model. The employed strategies and generated compounds could pave the way to a new class of gut-specific oral peptide probes and therapeutics to study and combat chronic gastrointestinal disorders, an area with substantial unmet medical needs.

INTRODUCTION

Recurrent and diffuse pain from the gut is the most dominant and disruptive symptom associated with functional gastrointestinal disorders such as irritable bowel syndrome (IBS).[1, 2] With a global prevalence of ~11%, IBS impairs the quality of life of millions of people and poses a serious economic burden on healthcare systems.[2, 3, 4] Abdominal pain is also a malicious feature in both acute and remission states of inflammatory bowel diseases (IBD, including ulcerative colitis and Crohn's disease),[5, 6] potentially life-threatening chronic conditions of unknown aetiology that affect ~0.5-1% in Western societies.[7] Adequate pain management in IBS and IBD care remains a complex endeavour that involves psychological, physical, dietary and pharmacological interventions, though often with limited success.[2, 8, 9] In particular, traditional analgesics such as nonsteroidal anti-inflammatory drugs (NSAIDs) and opioids are poorly effective, associated with adverse side effects, and can even enhance gastrointestinal disease progression.[10, 11] The increasing global prevalence of IBS- and IBD-related pain conditions and lack of broadly applicable treatment options are urging the need to establish and validate new therapeutic strategies that offer better management of abdominal pain.

Emerging evidence supports the oxytocin receptor (OTR) as a novel drug target within the gut with therapeutic value in chronic abdominal pain and gastrointestinal disorders.[12, 13, 14] OTR is a rhodopsin-like/class A G protein-coupled receptor (GPCR) belonging to a small subgroup of the closely related oxytocin (OT) and vasopressin (VP) GPCR family (OTR, $V_{1a}R$, $V_{1b}R$, V_2R).[14, 15] Activation of OTR by its endogenous ligand, the neurohypophyseal peptide OT, mediates essential physiological and psychological processes in the peripheral and central nervous systems, including reproductive functions (e.g., parturition, lactation), emotional functions (e.g., anxiety, stress, pain relief) and complex social behaviour (e.g., maternal and pair bonding, empathy, trust).[14, 16] OT/OTR expression also occurs in the gut,[17, 18, 19] where its role is less understood. Cumulative evidence suggests that OT/OTR signalling is involved in the development, maintenance and function of the gastrointestinal system,[17, 20] including regulation of gut motility,[21, 22, 23, 24] inflammation[25, 26, 27, 28, 29, 30] and epithelial gut barrier integrity.[31, 32] Moreover, human[33, 34, 35, 36] and animal[12, 13, 37, 38, 39] studies support the involvement of OT/OTR in peripheral abdominal pain sensing. Low levels of endogenous OT in plasma are associated with chronic abdominal pain.[33, 34] In line with this, administration of exogenous OT increases pain perception thresholds in IBS patients (continuous injection),[35] and has positive effects on abdominal discomfort and pain under conditions of chronic constipation (intranasal delivery).[36] Importantly, local activation of OTR signalling at the level of the gut wall can intercept pain perception by reducing visceral hypersensitivity,[12, 13, 37, 38, 39] i.e., the enhanced responsiveness of colon innervating sensory afferent nerves (nociceptors) to mechanical and chemical stimuli, a central mechanism underlying abdominal pain in IBS and IBD.[1, 2, 40] OTR expression is upregulated on colonic nociceptors[12] and mast cells[13] in animal (mice and rats) models of visceral hypersensitivity. Local luminal application (intra-colonic delivery) of OT and analogues to the gut wall reduces colonic nociceptor function[12, 37], reduces the number of neurons within the spinal cord that are activated by noxious colorectal distension[12] and triggers analgesia *in vivo*.[12, 13] Therefore, targeting OTR from the

luminal side of the epithelial lining with orally administered and gut-stable peptides represents an innovative and promising new gut-specific/restricted treatment approach for abdominal pain associated with IBS and IBD.

The digestive environment of the gastrointestinal tract constitutes a major stability challenge for oral peptide drug delivery.[41, 42] OT is stable to strongly acidic conditions and pepsin degradation in the stomach ($t_{1/2}$ >24 h), but rapidly degraded by pancreatic peptidases that are secreted to the lumen of the intestine ($t_{1/2}$ <10 min).[42, 43, 44] The nonapeptide sequence of OT consists of a 6-residue N-terminal cyclic moiety with a single disulfide bond and an amidated 3-residue C-terminal tail (Figure 1A). This structure is evolutionarily highly conserved,[14, 45, 46] rendering chemical efforts to improve its drug-like properties, such as metabolic stability, inherently challenging. Since its first chemical synthesis by Vincent du Vigneaud in 1953,[47, 48] OT has become one of the most studied peptides in the literature, with countless synthetic analogues revealing a complex structure-activity-relationship where even minor modifications can eradicate biological activity or trigger agonist-to-antagonist switches.[14, 49, 50, 51, 52] For instance, frequently applied strategies to improve the metabolic stability of peptides, such as the incorporation of D-amino acids,[53, 54, 55, 56, 57, 58, 59] N_{α}-methylation,[60] truncation,[61, 62, 63] cyclization,[56, 64, 65] scaffold grafting,[42] or N-terminal acetylation[66] are not well tolerated by the OT pharmacophore, resulting in inactivation. The structural integrity of the disulfide-cyclic N-terminal moiety of OT is crucial for OTR binding and activation.[67, 68] Reductive ring-opening by thiol-containing molecules or thiol oxidoreductases is a metabolic key pathway that causes inactivation (inactive linear dihydro-OT).[69, 70] Multiple non-reducible disulfide-bond mimetics have been proposed for OT, including dicarba,[71] lactam,[72] ether,[73] sulfone/sulfoxide[74] and stapled analogues (*via* xylene bridges[75] and thioacetal[76]). However, only subtle structural alterations *via* close disulfide surrogates that do not contract or extend OT's ring size, such as thioether-, diselenide- or selenoether-bonds, can fully retain bioactivity.[12, 56] Poor OTR selectivity of OT against the closely related VPRs poses another challenge in developing OTR-specific analogues.[14, 77, 78] Besides native OT, only two synthetic peptide analogues have reached clinical use as OTR agonists to date: demoxytocin (1-desamino OT, dOT; buccal or injection for labour induction)[79, 80, 81] and carbetocin (1-carba-1-desamino-2-O-methyl-tyrosine OT; injection for postpartum haemorrhage treatment).[82, 83, 84] While these compounds display some favourable properties such as extended circulation half-life, increased potency (dOT) or heat stability (carbetocin), they remain equally prone to degradation in the gastrointestinal environment as native OT.[42, 85, 86, 87]

Considering the therapeutic potential that gut-specific targeting of OTR holds for individuals suffering from chronic abdominal pain, we set out to develop the first series of potent and gut-stable OT analogues. We pursued a rational ligand design approach guided by mechanistic insights into OT's molecular degradation in intestinal fluid. This led to strategic and subtle site-specific modifications to improve ligand stability while retaining bioactivity. Following this structure-gut-stability-activity-guided strategy, we selected a potent and stable lead compound and evaluated its efficacy as an oral and gut-specific analgesic in a well-established mouse model of chronic abdominal pain.

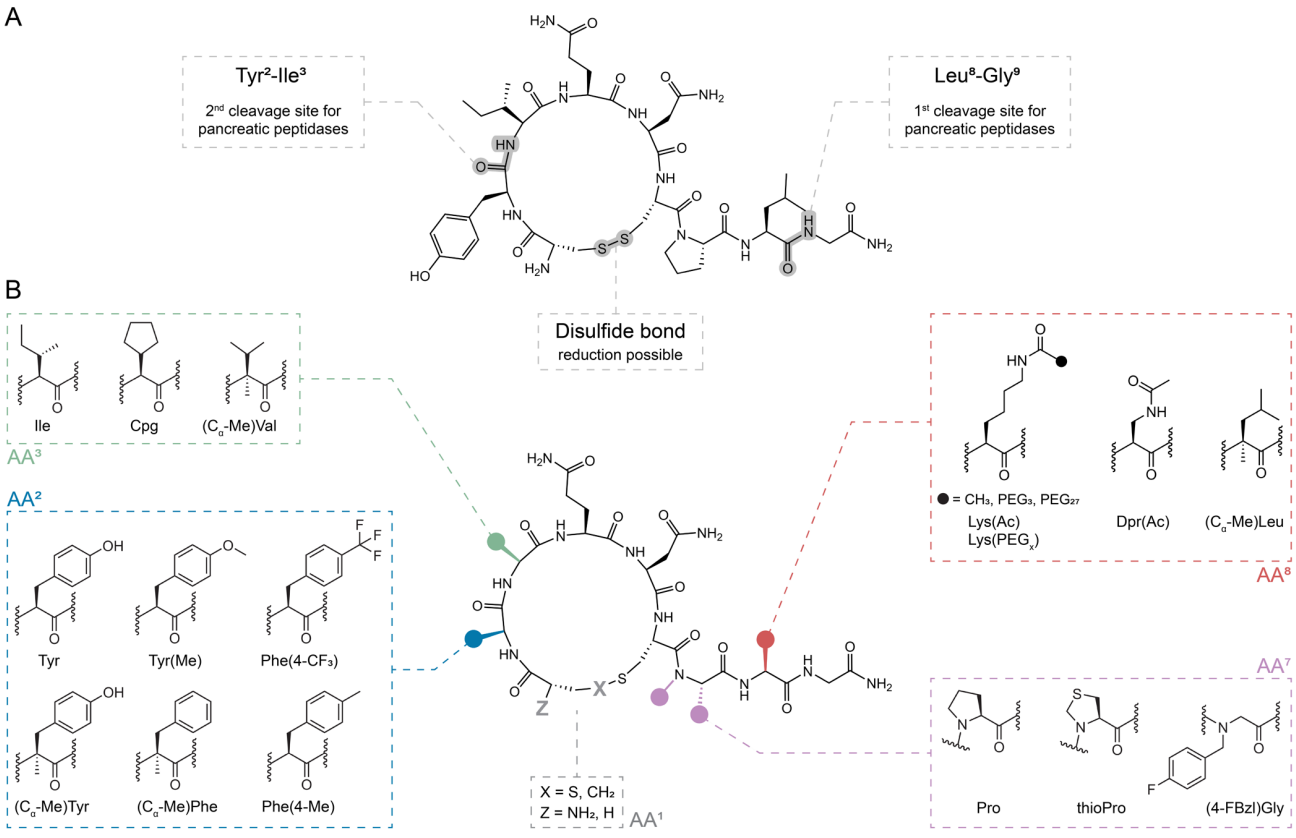

Figure 1: Rational design of oxytocin (OT) analogues with improved gastrointestinal stability. **A.** Chemical structure of native OT. Observed metabolic cleavage sites in intestinal fluid are indicated in grey. **B.** Chemical modification sites and strategies explored for the development of gut-stable OT analogues. Amino acid (AA) side-chain residues in positions 1, 2, 3, 7 and 8 were critical for developing gut-stable compounds. Structures of side-chain modifications explored for these critical positions are illustrated. The strategic combination of these modifications led to the development of compounds **1-28**, detailed in Table 1.

RESULTS

Fundamentals of analogue design: the intestinal metabolism of OT. Metabolism of OT in intestinal fluid (Figure 1A) proceeds *via* a step-wise cleavage of peptide bonds from the C-terminal tail,[42, 43] yielding truncated metabolites with reduced activity.[61, 62, 63, 88] Removal of the C-terminal Gly^9-amide, Leu^8Gly^9-dipeptide or complete tripeptide tail diminishes uterotonic activity[61, 63, 88] and C-terminally truncated OT and dOT analogues also have reduced potency (e.g., $desGly^9$-dOT ~45-fold less potent than OT/dOT).[62] The Tyr^2-Ile^3 interface is the second major cleavage site, which is recognised by pancreatic chymotrypsin, causing inactivation by opening the ring moiety.[89] This cleavage site is particularly favoured in analogues lacking an N-terminal amine or with a stabilised C-terminal tail.[42, 86, 87, 89] Guided by these degradation mechanisms, we devised site-specific chemical modifications to prevent the digestive degradation of OT while retaining bioactivity (Figure 1B). All analogues were synthesised using manual Fmoc-solid-phase peptide synthesis (Fmoc-SPPS),[90] characterised in terms of stability in simulated intestinal fluid (SIF)[42, 91] and functional activity at the human OTR and closely related $V_{1a}R$ (most relevant VP receptor for undesired cardiovascular side effects)[14, 78, 92] *via* well-established inositol-1-phosphate (IP-1) accumulation and FLIPR Ca^{2+}-mobilization assays.[78]

Design and characterisation of 1st generation analogues: modifications at position 8 to improve OT gut stability while retaining bioactivity. To intercept the initiation of OT's metabolism in the gut through the removal of Gly^9-amide, we first turned our attention towards stabilising the C-terminal tail by modifying position 8. We designed a series of analogues substituting Leu^8 to Lys^8 and used this as a handle to introduce various PEGylation motifs (**1-3**, Table 1). PEGylation can improve the stability of peptides and proteins by preventing access of digestive enzymes to cleavable bonds[93, 94] and introducing Lys or other handles in position 8 for modification of OT and analogues is well tolerated in terms of bioactivity.[14, 37, 95, 96, 97, 98, 99, 100, 101] The resulting compounds were stable to C-terminal degradation and revealed a ~50-fold SIF half-life improvement compared to OT. No considerable stability differences between PEGylation motifs of various lengths and complexity were observed (i.e., PEG_3 ~3xPEG_3 ~PEG_{27}). By contrast, the same modification strategies were not as successful in analogues lacking the N-terminal amino group (**6-9**, Table 1), highlighting that the second main recognition site of pancreatic chymotrypsin (Tyr^2-Ile^3) is cleaved at a faster rate in dOT than OT.[86, 87] These results also indicated that the non-canonical nature of the introduced PEGylated residues rather than steric hindrance prevented enzymatic cleavage at the C-terminal tail. We therefore simplified the modification approach and accessed compounds with acetylated instead of PEGylated side-chains in position 8 (**4**-**5**, Table 1). Indeed, two variants containing a $Lys(Ac)^8$ residue (**4**) or a shorter $Dpr(Ac)^8$ (diaminopropionic acid) moiety (**5**) were both devoid of C-terminal cleavage in SIF and revealed similar half-life improvements compared to the more complex, PEGylated analogues. Pharmacological evaluation on OTR activation revealed that all compounds were full agonists at OTR, close to or equipotent to native OT (Table 1 and S1, 1st generation). Only analogue **3** containing a large PEG_{27} moiety had ~10-fold reduced potency.

Table 1: Chemical structure information, intestinal gut-stability half-lives, and potency at the human oxytocin receptor of synthesised compounds.

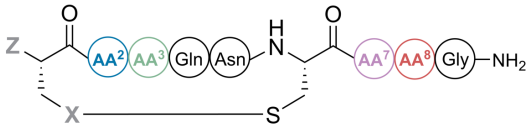

Compound	Z	X	AA^2	AA^3	AA^7	AA^8	SIF stability $t_{1/2}$	OTR potency fold change[(b)]
OT	NH_2	S	Tyr	Ile	Pro	Leu	8 ± 1 min[(a)]	1.0
dOT	H	S	Tyr	Ile	Pro	Leu	n.d.	0.3
Carbetocin	H	CH_2	Tyr(Me)	Ile	Pro	Leu	13 ± 1 min[(a)]	5.2
1st generation								
1	NH_2	S	Tyr	Ile	Pro	Lys(PEG_3)	6.8 ± 1.3 h	1.4
2	NH_2	S	Tyr	Ile	Pro	Lys[PEG_3(Lys(PEG_3)$_2$]	8.0 ± 0.7 h	1.9
3	NH_2	S	Tyr	Ile	Pro	Lys(PEG_{27})	5.6 ± 0.7 h	10
4	NH_2	S	Tyr	Ile	Pro	Lys(Ac)	5.4 ± 0.5 h	0.9
5	NH_2	S	Tyr	Ile	Pro	Dpr(Ac)	8.5 ± 0.5 h	2.4
6	H	S	Tyr	Ile	Pro	Lys(PEG_3)	21 ± 2 min	3.1
7	H	S	Tyr	Ile	Pro	Lys(PEG_{27})	18 ± 2 min	n.d.
8	H	S	Tyr	Ile	Pro	Lys[Lys(PEG_3)$_2$]	40 ± 5 min	2.2
9	H	S	Tyr	Ile	Pro	Lys[Lys(PEG_{27})$_2$]	35 ± 3 min	n.d.
2nd generation								
10	H	CH_2	Tyr(Me)	Ile	Pro	Lys(Ac)	>24 h	1.8
11	H	CH_2	Tyr(Me)	Ile	Pro	Dpr(Ac)	>24 h	30*
12	H	CH_2	Tyr(Me)	Ile	Pro	(C_α-Me)Leu	>24 h	18
13	H	CH_2	Phe(4-Me)	Ile	Pro	Dpr(Ac)	2.4 ± 0.2 h	4.9*
14	H	CH_2	Phe(4-CF_3)	Ile	Pro	Dpr(Ac)	>24 h	inactive
15	H	CH_2	(C_α-Me)Tyr	Ile	Pro	Lys(Ac)	>24 h	9.1
16	H	CH_2	(C_α-Me)Tyr	Ile	Pro	Dpr(Ac)	>24 h	65*
17	H	CH_2	(C_α-Me)Phe	Ile	Pro	Dpr(Ac)	>24 h	inactive
18	H	CH_2	Tyr	(C_α-Me)Val	Pro	Lys(Ac)	>24 h	31
19	H	CH_2	Tyr	(C_α-Me)Val	Pro	Dpr(Ac)	>24 h	280
20	H	CH_2	Tyr	Cpg	Pro	Lys(Ac)	11 ± 1 min	0.1
21	H	CH_2	Tyr	Cpg	Pro	Dpr(Ac)	13 ± 1 min	0.6
3rd generation								
22	H	CH_2	Tyr(Me)	Cpg	Pro	Lys(Ac)	>24 h	1.7
23	H	CH_2	Tyr(Me)	Cpg	thioPro	Lys(Ac)	>24 h	1.0
24	H	CH_2	Tyr(Me)	Ile	thioPro	Lys(Ac)	>24 h	1.1
25	H	CH_2	Tyr(Me)	Ile	(4-FBzl)Gly	Dpr(Ac)	1.4 ± 0.1 h	inactive
26	H	CH_2	(C_α-Me)Tyr	Ile	thioPro	Lys(Ac)	>24 h	1.9
27	H	CH_2	(C_α-Me)Tyr	Cpg	thioPro	Lys(Ac)	>24 h	3.1
28	H	CH_2	Tyr	(C_α-Me)Val	thioPro	Lys(Ac)	>24 h	14

[(a)] SIF stability of OT and carbetocin were previously reported and SIF stability assay protocols were kept identical.[42] [(b)][$EC_{50}{}^X$/$EC_{50}{}^{OT}$]: indicates fold potency reduction (values >1) or improvement (values <1) compared to OT; mean EC_{50} values of compounds (N=3 for IP-1, N=2 for FLIPR Ca^{2+}) were normalised to the mean EC_{50} of OT ($EC_{50}{}^{IP\text{-}1}$ = 2.56 ± 0.62 nM (N=9), $EC_{50}{}^{Ca2+}$ = 3.91 ± 0.87 nM (N=11). Inactive: E_{max} <25% up to 30 µM ligand concentration and/or EC_{50} >30 µM. *Partial agonist with E_{max} = 25-40%; all other compounds displayed E_{max} >85%; n.d.: not determined. Lead compounds of the 1st, 2nd and 3rd generations are highlighted by underlining. Please refer to SI for more detailed information, including EC_{50}, E_{max}, full concentration-response curves and full stability profiles of all analogues. Ac: acetyl; Cpg: L-cyclopentylglycine; dOT: 1-desamino OT; Dpr: L-diaminopropionic acid; (C_α-Me)Leu: α-methyl-L-leucine; Tyr(Me): O-methyl-L-tyrosine; (C_α-Me)Tyr: α-methyl-L-tyrosine; (4-FBzl)Gly: N-(4-fluorobenzyl)glycine; PEG: polyethylene glycol; (C_α-Me)Phe: α-methyl-L-phenylalanine; Phe(4-Me): 4-methyl-L-phenylalanine; Phe(4-CF_3): 4-(trifluoromethyl)-L-phenylalanine; thioPro: thiazolidine-4-carboxylic acid; (C_α-Me)Val: α-methyl-L-valine

Design and characterisation of 2nd generation analogues: strategic combination of modifications in position 8 and 2 or 3 yielding highly gut-stable and bioactive OT analogues. Metabolism of C-terminally stabilised 1st generation analogues in SIF exclusively proceeded *via* cleavage between Tyr^2-Ile^3 (Figure 1A), accompanied by ring-opening and subsequent excision of Tyr^2 (confirmed by HPLC-MS/MS analysis, Figure S1-S4). Modification of either of the two residues Tyr^2/Ile^3 at the cleavage site could impart stabilisation.

The chemical nature and side-chain configuration in position 2 of OT and analogues are essential for agonistic activity.[67, 102] Structural alterations to the backbone or side-chain of Tyr^2, such as N_α-methylation,[60] inversion of C_α configuration (D-Tyr^2),[54] or substitution with other canonical amino acids[103] typically eradicate activity or trigger agonist-to-antagonist switches. Despite extensive research, no modification for this position has yet been identified that entirely preserves or even improves functional potency,[49] indicating that engineering of this N-terminal moiety is particularly challenging. One successful example with an unnatural O-methylated Tyr(Me) residue in position 2 and a modified thioether-based N-terminal ring structure is clinically used carbetocin (Table 1).[82, 83, 84] Carbetocin undergoes a similar rapid C-terminal degradation in SIF as OT ($t_{1/2}^{SIF}$ = 13 ± 1 min),[42] but $Tyr(Me)^2$ can prevent chymotrypsin catalysed ring-opening[85] and, therefore, could stabilise the second major cleavage site of OT in intestinal fluid. In addition, the replacement of the disulfide bond with a non-reducible thioether linkage prevents any redox-associated metabolic pathways, as seen with other orally administered and disulfide-rich peptide drugs.[104]

We therefore combined the identified stabilising position 8 modifications from the 1st generation analogues ($Lys(Ac)^8$ and $Dpr(Ac)^8$) with carbetocin-like $Tyr(Me)^2$ and thioether cyclisation, hypothesising that the resulting compounds would resist degradation in SIF and maintain bioactivity of the parent compounds. Indeed, analogues **10** and **11** (Table 1) were highly stable in SIF ($t_{1/2}^{SIF}$ >24 h), with no major metabolites detected over 24 h. Interestingly, the pharmacological characterisation of OTR activation revealed a considerable difference between the $Lys(Ac)^8$ (**10**) and the $Dpr(Ac)^8$ (**11**) analogues. Compound **10** displayed almost full agonistic activity and a similar potency as OT (E_{max} = 86 ± 5 %, ~1.8-fold reduced potency), while the shorter $Dpr(Ac)^8$ side-chain in **11** resulted in reduced activity (E_{max} <40 %, ~30-fold reduced potency) (Table 1 and S1). These results were also comparable to analogue **12**, in which a stabilising C_α-backbone methylation at Leu^8 ($(C_\alpha$-Me)Leu^8)[42] was introduced instead of an acetylated side-chain, yielding a less potent but stable compound ($t_{1/2}^{SIF}$ >24 h, ~18-fold reduced potency). Since this modification would also reduce the synthetic flexibility for functional side-chain modifications in position 8 (e.g., labelling), we did not further pursue the $(C_\alpha$-Me)Leu^8 analogues.

Based on these results, we expanded the scope of tyrosine mimetics in position 2 beyond carbetocin-like Tyr(Me) modification to probe the boundaries for pharmacological and stability improvements (**13-17**, Table 1). Substitution of the methoxy moiety in $Tyr(Me)^2$ by a methyl group ($Phe(4\text{-}Me)^2$) did not retain stability in SIF (**13**, $t_{1/2}^{SIF}$ = 2.4 ± 0.2 h). By contrast, trifluoromethylation ($Phe(4\text{-}CF_3)^2$) of the

same position resulted in gut-stable analogue **14**, indicating that site-specific fluorination can promote gut stability. Analogue **14**, however, was inactive. Insertion of a C_α-methylation to the backbone of Tyr^2 ($(C_\alpha\text{-Me})Tyr^2$) also prevented cleavage by pancreatic peptidases and yielded gut-stable analogues **15** and **16** ($t_{1/2}^{SIF}$ >24 h). This modification was also well tolerated regarding bioactivity when combined with $Lys(Ac)^8$ (**15,** full agonist, ~9.1-fold reduced potency). By contrast, the combination of $(C_\alpha\text{-Me})Tyr^2$ with $Dpr(Ac)^8$ (**16**) resulted again in a considerable drop in activity (E_{max} <40 %, ~65-fold reduced potency compared to OT). The same trend was observed in gut-stable but inactive analogue **17**, in which the phenolic OH in position 2 ($(C_\alpha\text{-Me})Phe^2$) was additionally removed.

We then investigated keeping Tyr^2 unmodified while altering position 3 to stabilise the second major intestinal cleavage site. We designed and accessed compounds combining the C-terminal $Lys(Ac)^8$/$Dpr(Ac)^8$ modification with two non-canonical Ile^3 mimetics (**18**-**21**, Table 1). Introduction of $(C_\alpha\text{-Me})Val^3$ prevented degradation and yielded fully gut-stable analogues **18** and **19** ($t_{1/2}^{SIF}$ >24 h). With regards to bioactivity, $Lys(Ac)^8$-containing **18** was again superior (~31-fold reduced potency) to $Dpr(Ac)^8$ modified analogue **19** (~280-fold reduced potency). In a second subseries, we substituted Ile^3 with cyclopentyl glycine (Cpg^3)[105] to produce analogues **20** ($Lys(Ac)^8$) and **21** ($Dpr(Ac)^8$). Despite the non-canonical nature of Cpg^3, both analogues were readily degraded in SIF *via* cleavage between position 2 and 3 ($t_{1/2}^{SIF}$ <15 min; cleavage site confirmed *via* MS/MS analysis; Figure S5 and S6). Of note, analogue **20** was ~10-fold more potent compared to OT. Interestingly, $Dpr(Ac)^8$ was also better tolerated in this series (**21**, ~2-fold more potent compared to OT), suggesting that the combination of position 2 and 8 is crucial for potent activity and that $Dpr(Ac)^8$ is only tolerated with an unmodified Tyr at position 2, which was supported by the potent activity of compound **5** from the 1st generation of analogues.

Overall, analogues **10** ($Tyr(Me)^2$), **15** ($(C_\alpha\text{-Me})Tyr^2$) and **18** ($(C_\alpha\text{-Me})Val^3$) emerged as lead structures from the 2nd generation, all including distinct modifications in position 2 or 3 and displaying high gut stability ($t_{1/2}^{SIF}$ >24 h) and low nM activity.

Design and characterisation of the 3rd generation of analogues: lead optimisation. In a final quest to improve the pharmacological properties of the gut-stable lead structures (**10**, **15** and **18**), we combined the most promising strategies from the 2nd generation and included selected modifications at position 7 (Pro^7). Pro^7 acts as a hinge residue between the N-terminal cyclic moiety and the linear C-terminal tail of OT that determines the conformational *cis-trans* ratio of the two moieties and impacts both potency and selectivity *vs.* the closely related VPRs.[106] We therefore probed two different Pro^7 mimetics together with identified stabilising lead modifications: $thioPro^7$, which imparts a higher *trans* conformational content and improves OT activity,[107] and more recently discovered N-alkylated Gly derivative N-(4-fluorobenzyl)glycine ($(4\text{-FBzl})Gly^7$), which is a key modification in merotocin, a highly potent and OTR-selective OT analogue and clinical candidate for lactation support.[108] Besides gut stability and OTR activity, we also assessed $V_{1a}R$ activation for this final series (Table S1) to address functional selectivity *vs* this closely related receptor target.

Starting from lead compound **10**, substitution of Ile^3 to Cpg^3 did not advance ligand properties, with gut-stable analogue **22** ($t_{1/2}^{SIF}$ >24 h) having similar potency to OT (~1.7-fold reduced) and no functional selectivity enhancement *vs.* $V_{1a}R$ compared to **10** (Table S1). Further incorporation of thioPro^7, however, yielded two of the most interesting gut-stable analogues in the series: **23** and **24** were full agonists equipotent to OT (Table 2 and Figure 2; Figure S7A) and displayed only weak partial agonistic activity at $V_{1a}R$ (E_{max} <40%, Table 2, Figure 2). By contrast, the substitution of Pro^7 in **11** with (4-FBzl)Gly^7 resulted in an unstable and inactive analogue (**25**), which degraded in SIF *via* cleavage between the two chemically modified (non-canonical) residues in positions 7 and 8, further highlighting the digestive strength and complex stability hurdle that pancreatic peptidases impose on peptide drugs in the intestine.

Applying the same modification strategies (Cpg^3, thioPro^7) to lead structure **15** also advanced this series. Analogues **26** and **27** retained full stability in SIF and were significantly more potent than **15** (Figure 2A-B and Table 2, $p < 0.05$ compared to **15**, Figure S7B). Importantly, **26** also displayed good functional selectivity for OTR *vs.* $V_{1a}R$ (>20,000-fold), with no agonistic activity at $V_{1a}R$ up to 10 µM and only a minor response (E_{max} <50%) at 100 µM (Table 2 and Figure 2C).

Incorporation of thioPro^7 into lead structure **18** yielded compound **28,** which had significantly enhanced potency compared to **18** (Table 2, $p < 0.05$, Figure S7C). In contrast to other improved leads (**23**, **24** and **26,** Figure 2D), analogue **28** also activated $V_{1a}R$, however, with reduced potency compared to OT (Table 2 and Figure 2C).

Figure 2E provides a schematic overview of the development of the three generations of OT analogues with regard to gut stability (SIF) and potency (OTR) relative to OT. Analogue **26** (Figure 2D) was selected for *in vivo* studies in a mouse model of chronic abdominal pain.

Table 2: Pharmacological characterisation, functional receptor selectivity and intestinal stability of leads.

Compound	OTR		$V_{1a}R$		OTR functional selectivity	$t_{1/2}^{SIF}$
	EC_{50} [nM]	E_{max} [%]	EC_{50} [nM]	E_{max} [%]		
OT	2.56 ± 0.62	100	21.7 ± 5.00	97 ± 3	8	8 ± 1 min[(a)]
Carbetocin	13.4 ± 3.31	94 ± 3	inactive		>7500	13 ± 1 min
VP	60.8 ± 28.0	93 ± 5	0.70 ± 0.57	100	–	< 3 min[(a)]
23	2.56 ± 0.51	93 ± 7	62.8 ± 2.36	38 ± 4	25	>24 h
24	2.80 ± 0.66	91 ± 9	84.6 ± 20.1	25 ± 2	30	>24 h
26	4.90 ± 1.97	102 ± 2	inactive		>20,000	>24 h
28	35.0 ± 3.71	108 ± 6	1051± 155.0	97 ± 3	30	>24 h

[(a)] SIF stability under identical assay conditions previously reported.[42] [(b)] OTR functional selectivity: [$EC_{50}^{V1aR}/EC_{50}^{OTR}$]; for 'inactive' compounds functional selectivity was calculated based on the highest concentration tested at $V_{1a}R$. IP-1 accumulation data is shown; compounds were tested up to 10 µM ligand concentration at OTR and 100 µM at $V_{1a}R$; N ≥ 3, N ≥ 3, mean ± SEM; 'inactive': E_{max} < 25% up to 100 µM at $V_{1a}R$; IP-1 data of all compounds were normalised to OT at OTR and VP at $V_{1a}R$ respectively.

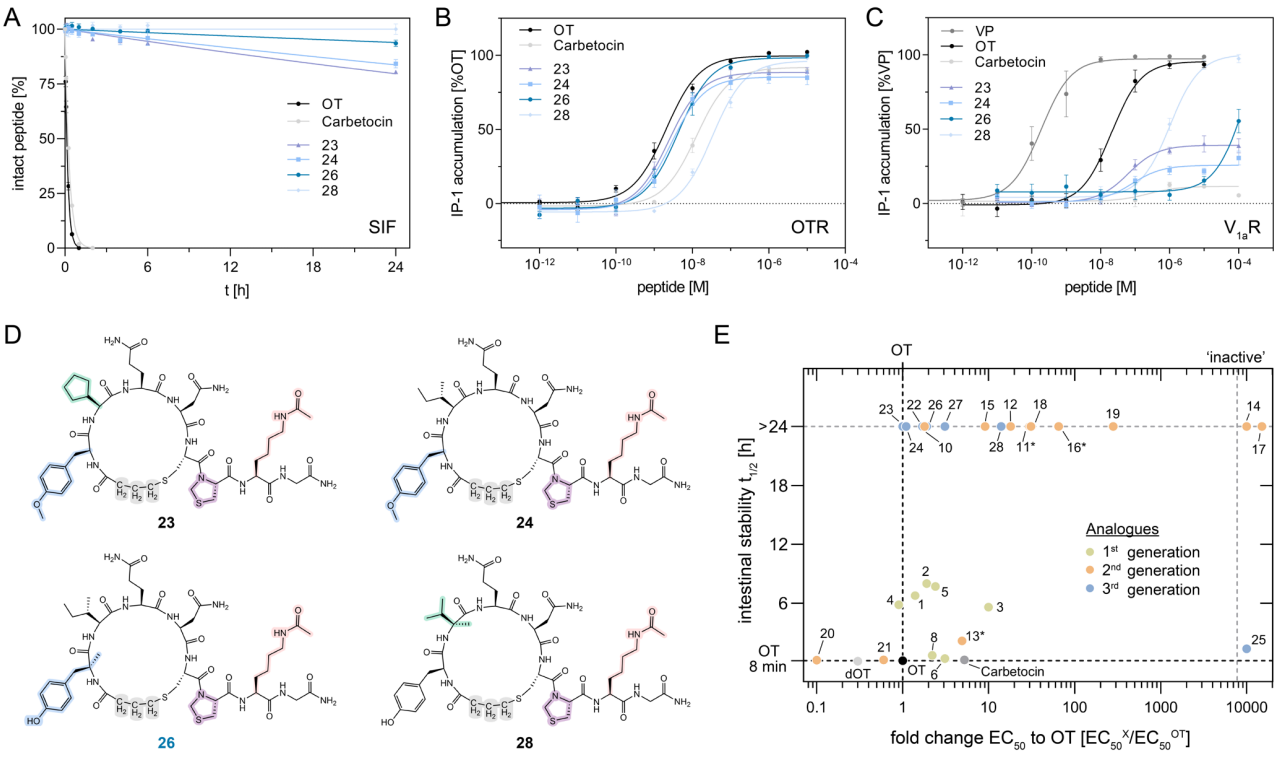

Figure 2: *In vitro* gut stability and potency of developed OT analogues and final 3rd generation lead structures. A. Full stability curves of lead compounds in SIF over 24 h (N=3, mean ± SEM). **B.** Full concentration-response curves of lead compounds at human OTR (IP-1 accumulation data, N ≥ 3, mean ± SEM). **C.** Full concentration-response curves of lead compounds at human $V_{1a}R$ (IP-1 accumulation data, N ≥ 3, mean ± SEM). **D.** Chemical structures of gut-stable lead compounds. **E.** Schematic overview on the gut stability and potency of three generations of OT analogues ('structure-gut-stability-activity-relationship-study', colour-coded). Each dot represents one developed compound (Table 1) mapped according to its SIF half-life ($t_{1/2}$) and potency at OTR. The EC_{50} value of each analogue was normalised to the EC_{50} of OT (EC_{50}^{X}/EC_{50}^{OT}) and is indicated as 'fold change EC_{50} to OT'. Mean values are presented (n ≥ 2). Compounds displaying E_{max} <25% up to 30 µM ligand concentration and/or EC_{50} >30 µM (>7,700-fold compared to OT) were defined as 'inactive'. *Partial agonist with E_{max} = 25-40%; all other compounds displayed E_{max} >85%. Black dashed lines highlight the stability and potency of native OT. Grey dashed lines indicate the experimental borders of stability (24 h) and activity assays.

***In vivo* characterisation: gut-stable OT analogue 26 triggered analgesia in a mouse model of chronic abdominal pain.** We previously demonstrated that OT and OT analogues reduce colonic nociceptor responses to mechanical stimuli in chronic visceral hypersensitivity (CVH) but not in healthy mice.[12, 37] This is a result of a considerable upregulation of OTR expression on colonic nociceptors in CVH states.[12] Therefore, in the current study, we focused on testing the analgesic potential of gut-stable analogue **26** in CVH. Figure 3A provides a schematic overview of the CVH model and the intra-colonic dosing paradigm of analogue **26**.

Measuring the visceromotor response (VMR) to colorectal distension (CRD) in the same mouse following intra-colonic vehicle and analogue **26** allowed us to compare changes in VMR within individual animals as well as across groups. Intra-colonic dosing of analogue **26** at 3.5 µg/kg (1 µM) significantly reduced pain responses to CRD in CVH mice compared with those treated with vehicle (Figure 3B). Pain responses were reduced by ~31% (Figure 3C), with significant reductions occurring

only at noxious distension pressures (Figure 3D). By increasing the intra-colonic concentration of analogue **26** to 350 µg/kg (100 µM) we observed significantly greater inhibition (Figure 3E) with a ~45% reduction in pain responses to CRD compared with vehicle (Figure 3F). Notably, the higher concentration of analogue **26** (350 µg/kg, 100 µM) inhibited pain responses to both non-noxious and noxious distension pressures (Figure 3G). These data indicate that the analgesic actions of analogue **26** are dose-dependent and that analogue **26** inhibits colonic afferents to reduce the VMR to CRD, as we have observed previously.[12, 37]

Based on these findings and the gut stability of analogue **26,** we pursued oral dosing relevant for therapeutic translation. We measured baseline pain responses to CRD in CVH and then dosed mice with two different oral doses of analogue **26** (2 mg/kg or 4 mg/kg) and measured pain responses 3.5-4 hours later (Figure 4A). Oral administration of 2 mg/kg analogue **26** did not significantly alter the VMR to CRD at non-noxious and noxious distension pressures (Figure 4B-D). However, oral delivery of analogue **26** at 4 mg/kg significantly reduced pain responses to CRD by ~26% compared with CVH baseline responses to CRD (Figure 4E-F). Notably, analogue **26** at 4 mg/kg significantly reduced responses to both non-noxious and noxious distension pressures (Figure 4G). Overall, these data support analogue **26** as an orally active analgesic acting locally in the gut *via* inhibition of colonic nociceptors.

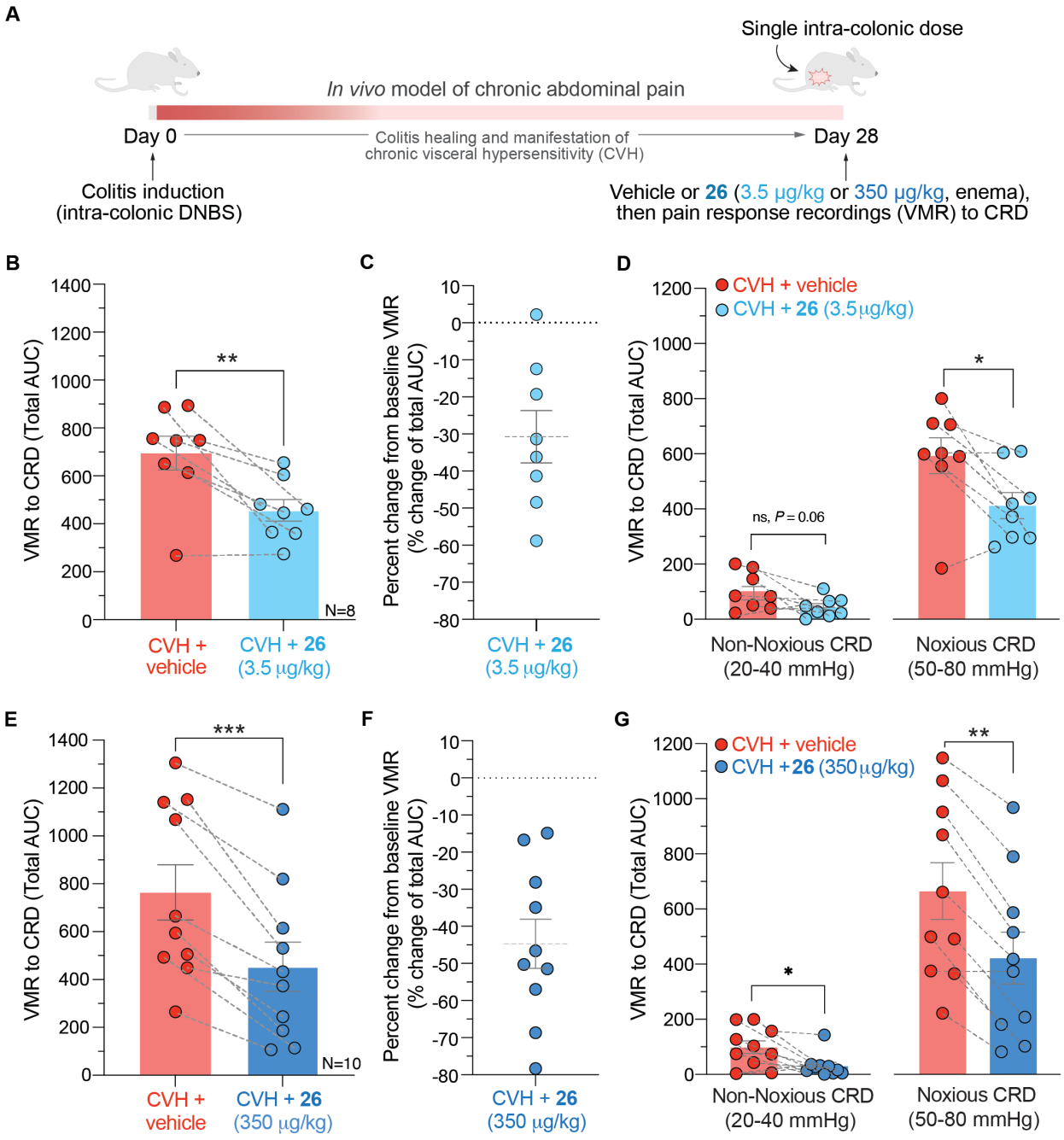

Figure 3: *In vivo* intra-colonic delivery of analogue 26 reduces abdominal pain to colorectal distension (CRD) in chronic visceral hypersensitivity (CVH) mice. A. Schematic illustration of the time course of the CVH mouse model and intra-colonic dosing of analogue **26** at either 3.5 µg/kg (equivalent to 1 µM) or 350 µg/kg (equivalent to 100 µM) for visceromotor response (VMR) studies to CRD. **B.** Total area under the curve (AUC) of the VMR to CRD showing intra-colonic administration of analogue **26** (3.5 µg/kg, 1 µM) significantly reduces pain responses in CVH mice compared with those treated with vehicle (**p <0.01, paired t-test, N=8). Each dot represents the combined VMR across all CRD pressures for an individual mouse. The dashed line indicates before and after analogue **26** comparisons for each mouse. **C.** Percentage change from baseline response indicating an overall ~31% reduction in VMR with intracolonic 3.5 µg/kg (1 µM) analogue 26. **D.** VMR to CRD at non-noxious and noxious CRD pressures, showing intra-colonic administration of analogue **26** 3.5 µg/kg (1 µM) significantly reduces pain responses at noxious CRD pressures (*p <0.05, Wilcoxon matched-pairs, N=8). Each dot represents the combined VMR across those pressures indicated for an individual mouse. **E.** Intra-colonic administration of analogue **26** (350 µg/kg, 100 µM) significantly reduces pain responses in CVH mice compared with those treated with vehicle (***p <0.001, paired t-test, N=10). **F.** Intra-colonic administration of analogue **26** (350 µg/kg, 100 µM) reduced the overall VMR to CRD by ~45% compared with baseline. **G.** VMR to CRD at non-noxious and noxious CRD pressures, showing intra-colonic administration of analogue **26** (350 µg/kg, 100 µM) significantly reduced pain responses at non-noxious (*p <0.05, paired t-test, N=10) and noxious CRD pressures (**p <0.01, Wilcoxon matched-pairs, N=10).

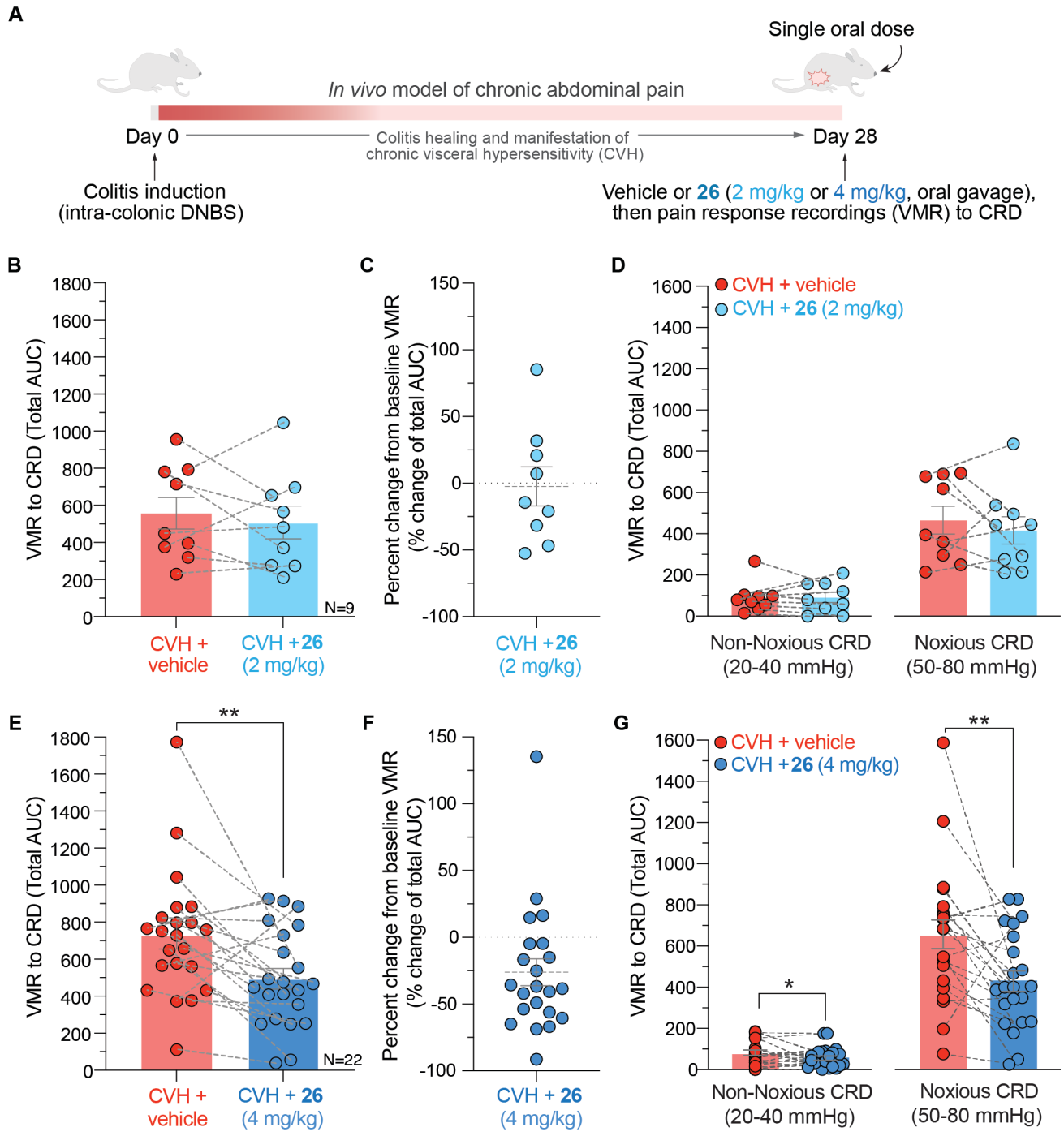

Figure 4: *In vivo* oral administration of analogue 26 reduces abdominal pain to colorectal distension in CVH mice. A. Schematic illustration of the time course of the CVH model and oral dosing of analogue **26** at either 2 mg/kg or 4 mg/kg for VMR studies to CRD. **B.** Total area under the curve (AUC) of the VMR to CRD showing oral administration of analogue **26** (2 mg/kg) did not significantly alter pain responses in CVH mice compared with those treated with vehicle (ns, p>0.05, paired t-test, N=9). Each dot represents the combined VMR across all CRD pressures for an individual mouse. The dashed lines indicate before and after analogue 26 comparisons for each mouse. **C.** Percentage change from baseline response indicating ~2% change in VMR to CRD with oral 2 mg/kg of analogue **26**. **D.** VMR to CRD showing oral administration of analogue **26** (2 mg/kg) did not significantly alter pain responses at non-noxious (ns, p>0.05, paired t-test, N=9) or noxious CRD pressures (ns, p>0.05, paired t-test, N=9). **E.** Oral administration of analogue **26** (4 mg/kg) significantly reduced pain responses in CVH mice compared with those treated with vehicle (**p <0.01, paired t-test, N=22). **F.** Oral administration of analogue **26** (4 mg/kg) reduced the overall VMR to CRD by ~26% compared with CVH baseline. **G.** VMR to CRD showing oral administration of analogue **26** (4 mg/kg) significantly reduced pain responses at non-noxious (*p < 0.05, Wilcoxon test, N=22) and noxious (**p < 0.01, Wilcoxon test, N=22) CRD pressures.

DISCUSSION

Adequate pain management is a critical challenge in the care of IBS and IBD, which are major clinical forms of abdominal pain. Common analgesic drugs are of limited use, often failing to provide the required long-term efficacy and safety profiles. Classical NSAIDs (e.g., aspirin, rofecoxib) or paracetamol, for instance, provide little or no relief in abdominal pain and their long-term use is associated with multiple gastrointestinal pathologies (e.g., constipation, epithelial damage and enhanced permeability, colitis, ulcers).[109] Moreover, misuse of centrally acting opioids (conventional μ-opioids, e.g., oxycodone, morphine) in patients with chronic abdominal pain has substantially contributed to the emergence of the current opioid crisis, despite lacking robust evidence for efficacy in gut pain and well-established destructive consequences,[10, 11] further exemplifying the pressing demand for new treatment strategies. We report here the development of a new generation of potent and highly gut-stable peptides that represent a stepping stone towards exploiting OTR as an orally accessible and gut-specific drug target in chronic abdominal pain and gastrointestinal disorders.

The engineering of metabolically stable variants of therapeutic sequences is a recognized challenge in peptide drug development[110, 111, 112] since chemical modifications that confer stability often abolish target binding and activation. This balance between molecular stabilization and retained bioactivity is particularly demanding in short and evolutionarily well-conserved sequences such as OT-like neuropeptides, where most residues are involved in receptor binding and activation[67, 102, 113] and common stabilization strategies often fail to produce active ligands.[42, 53, 54, 55, 56, 57, 58, 59, 60, 61, 62, 63, 64, 65, 66] Substantial efforts have been made to create long-acting (more stable) OT analogues focusing on enhancing plasma circulation half-life upon injection.[95, 96, 100, 114, 115] Gut-targeted activity, however, requires peptides to resist degradation in the considerably more complex digestive environment of the gastrointestinal tract.[42] While the stomach (acidic pH, pepsin) is less of a hurdle for OT (and many other peptides), pancreatic peptidases in the lumen of the intestine efficiently degrade most peptides (OT: $t_{1/2}^{SIF}$ = 8 ± 1 min).[42, 43, 44] To address this, we applied a step-wise ligand design approach guided by structure-gut-stability-activity-relationship data, installing subtle alterations to the OT pharmacophore. Site-specific modifications in four positions (1, 2 or 3, 7 and 8) of the 9-mer native OT sequence were crucial for the development of potent and gut-stable analogues. The introduction of an acetylated lysine side-chain in position 8 ($Lys(Ac)^8$) was key to effectively preventing C-terminal truncation in intestinal fluid while retaining bioactivity. The strategic combination of $Lys(Ac)^8$ with modification of Tyr^2 or Ile^3 provided strong stability improvement in SIF. Besides carbetocin-like O-methylated $Tyr(Me)^2$, site-specific C_α-backbone methylation (in positions 2 and 3) was a well-tolerated modification for these critical residues, preserving bioactivity and preventing intestinal degradation. To counteract metabolic inactivation *via* reductive-ring opening by redox-active molecules and enzymes in the gut, we also substituted native disulfide-cyclization with a non-reducible thioether linkage.[116] Further combination of these stabilizing modifications with a proline mimetic in position 7 ($thioPro^7$) resulted in better functional selectivity for OTR *vs* $V_{1a}R$ and improved the potency of lead

compounds (**26** and **28**, Figure S7).[107] These modification strategies yielded a new and first series of highly gut-stable and potent OT analogues.

Intra-colonic administration of a single dose of gut-stable lead analogue **26** triggered significant analgesia in mice with CVH. These effects resulted from a short-time application (30 min) directly to the gut wall, pointing to topical accessibility of OTR from the luminal side of the mucosa. We also observed that these analgesic effects were dose-dependent and that oral administration of the gut-stable lead analogue **26** induced analgesia in CVH mice 3.5-4 hours after administration. Overall, these data align with previous results suggesting that a local pain-modulating (anti-nociceptive) effect of gut-specific OTR activation could be mediated by two presumably synergistic mechanisms. First, during CVH (but not in healthy controls), OTR is upregulated on the peripheral endings of colonic sensory afferents, and activation of OTR signalling directly on receptor-expressing sensory neurons then inhibits nociceptive signalling in the spinal cord, resulting in reduced pain perception to noxious stimuli.[12] Second, in states of visceral hypersensitivity, OTR is also overexpressed on colonic mast cells, and local receptor activation inhibits mast cell degranulation,[13] thereby preventing the release of pro-nociceptive mediators that drive visceral hypersensitivity.[117]

Indeed, reducing or preventing peripheral sensitization (visceral hypersensitivity) is increasingly emerging as a seminal concept in abdominal pain treatment, tackling a key mechanism underlying pain perception in IBS and IBD.[1, 2, 40, 109] Peptides are innovative candidates for drug development in this context since their inherently low systemic uptake (i.e., 'gut-restriction' due to poor absorption through the epithelial lining; oral bioavailability typically <1%) paired with a gut-located target enables a non-systemic, gut-specific treatment approach with a high safety profile (due to reduced risk of systemic effects). Blockbuster drug linaclotide (14-mer with three disulfide bonds), targeting from the gut-lumen accessible guanylate cyclase-C (GC-C) receptors, is a front-runner of this novel class of oral peptide drugs that remain restricted to the gut-lumen (<0.1% oral bioavailability).[104, 118, 119] GC-C receptor activation improves gastrointestinal transition and also inhibits colonic nociceptor function, thus relieving abdominal pain in patients with constipation-predominant IBS (IBS-C) and chronic idiopathic constipation.[120, 121, 122, 123] Our work strengthens the evidence for a strong therapeutic potential of local gut-specific OTR activation in abdominal pain treatment. Importantly, since exogenous OT has no effect on nociception in CVH-free mice (intra-colonic application; corresponding with a lack of afferent OTR overexpression)[12] nor thresholds of abdominal pain perception in healthy human individuals (injection),[21] delivery of stable OT analogues to the gut lumen could target a unique local and disease-associated therapeutic window. Such locally acting analgesics could suppress the pain signal at the site of origin, providing pain relief without risking undesired systemic or even central (side) effects (e.g., μ-opioids).

In view of this gut-targeted mode of action, sufficient stability to digestive degradation is key for orally active peptide drugs. Specifically, high molecular stability can result in safer therapeutic applications (due to, e.g., lower dosing and fewer metabolites, both reducing potential off-target effects), and also

removes the necessity for drug formulation (e.g., co-formulation of enzyme inhibitors or pH regulators) or advanced delivery-strategies (e.g., encapsulation, slow-release technologies).[41, 124, 125, 126] The latter is complex and can hardly account for the frequently varying physiological conditions in the gastrointestinal tract (i.e., depending on age, gender, health condition and daytime).[127, 128] The new series of OT analogues introduced in this work fulfil this criterion and are highly gut-stable, even when challenged with enhanced (4-times) digestive strength conditions (Figure S8).

CONCLUSION

We have chemically engineered a first series of gut-stable and potent OT analogous as therapeutic lead compounds in abdominal pain and chronic gastrointestinal disorders. Considering the complex structure-activity-relationship of this neuropeptide, the outlined strategic ligand design concepts might also be relevant for developing gut-stable variants of similarly challenging target sequences. We demonstrated that a single intra-colonic dose of a gut-stable lead triggered significant local and dose-dependent analgesic effects in a chronic abdominal pain mouse model. Furthermore, oral administration of the gut-stable lead also triggered significant analgesic effects, laying a strong foundation to pursue OTR as a novel orally accessible drug target in debilitating chronic gastrointestinal disorders such as IBS and IBD.

EXPERIMENTAL SECTION

Materials.

All reagents and solvents were commercially obtained in analytical or peptide synthesis grade and used without further purification.

Peptide Synthesis. Standard protected 9-Fluorenylmethoxycarbonyl (Fmoc)-amino acids, Fmoc-S-p-methoxytrityl-L-cysteine (Fmoc-Cys(Mmt)-OH, CAS: 177582-21-7), Boc-S-trityl-L-cysteine (Boc-Cys(Trt)-OH, CAS: 21947-98-8), Fmoc-alpha-methyl-L-phenylalanine (Fmoc-(C_α-Me)Phe-OH, CAS: 135944-05-7), 3-Trityl-mercaptopropionic acid (Mpa(Trt), CAS: 27144-18-9), Fmoc-L-thiazolidine-4-carboxylic acid (Fmoc-thioproline, Fmoc-thioPro-OH, CAS: 133054-21-4), Fmoc-NH-PEG_3-COOH (CAS: 867062-95-1), N,N'-diisopropylcarbodiimide (DIC), Oxyma Pure and Fmoc-Rink amide AM resin (0.74 mmol/g, 100-200 mesh) were purchased from Iris Biotech GmbH (Marktredwitz, Germany). TentaGel R RAM (Rink amide) resin (0.19 mmol/g, particle size: 90 µm) was purchased from Rapp Polymere (Tübingen, Germany). 1-[Bis(dimethylamino)methylene]-1H-1,2,3-triazolo[4,5-b]pyridinium 3-oxide hexafluorophosphate (HATU), 4-bromobutyric acid (CAS: 2623-87-2), phenylsilane ($PhSiH_3$), Fmoc-L-cyclopentylglycine (Fmoc-Cpg-OH, CAS: 220497-61-0), Fmoc-alpha-methyl-L-leucine (Fmoc-(C_α-Me)Leu-OH, CAS: 312624-65-0), Fmoc-O-methyl-L-tyrosine (Fmoc-Tyr(Me)-OH, CAS: 77128-72-4), Fmoc-(4-trifluoromethyl)-L-phenylalanine (Fmoc-Phe(4-CF_3)-OH, CAS: 247113-86-6) and 4-fluorobenzylamine (CAS: 140-75-0) were purchased from Fluorochem Ldt. (Derbyshire, UK). Dichloromethane (DCM), N,N-dimethylformamide (DMF), diethyl ether (Et_2O), ethyl acetate (EtOAc), heptane and trifluoroacetic acid (TFA) were purchased from VWR International

(Darmstadt, Germany). Piperidine, N,N-diisopropylethylamine (DIEA), triisopropylsilane (TIPS), 3,6-dioxa-1,8-octane-dithiol (DODT), dimethyl sulfide (DMS), 4-bromobutyryl chloride (CAS: 927-58-2), Fmoc-N-ε-acetyl-L-lysine (Fmoc-Lys(Ac)-OH, CAS: 159766-56-0), Fmoc-N-β-4-methyltrityl-L-diaminopropionic acid (Fmoc-Dpr(Mtt)-OH, CAS: 654670-89-0), Fmoc-N-ε-Fmoc-L-lysine (Fmoc-Lys(Fmoc)-OH, CAS: 78081-87-5), bromoacetic acid (CAS: 79-08-3) and allyl alcohol (CAS: 107-18-6) were purchased from Sigma-Aldrich, Merck (Darmstadt, Germany). Fmoc-N-ε-4-methyltrityl-L-lysine (Fmoc-Lys(Mtt)-OH, CAS: 167393-62-6) was purchased from GL Biochem (Shanghai, China). Fmoc-4-methyl-L-phenylalanine (Fmoc-Phe(4-Me)-OH, CAS: 199006-54-7) was purchased from Alfa Aesar, Thermo Fisher Scientific (Kandel, Germany), Fmoc-alpha-methyl-O-t-butyl-L-tyrosine (Fmoc-(C_α-Me)Tyr(tBu)-OH, CAS: 1309873-74-2) from Syntides, Psyclo Peptide (Shanghai, China) and Fmoc-alpha-methyl-L-valine (Fmoc-(C_α-Me)Val-OH, CAS: 169566-81-8) from Bachem (Bubendorf, Switzerland). Fmoc-NH-PEG_{27}-COOH (CAS: 15137-2790) was purchased from Polypure (Oslo, Norway). (Benzotriazol-1-yloxy)tripyrrolidinophosphonium hexafluorophosphate (PyBOP, CAS: 128625-52-5) was purchased from Carbosynth Ltd, (Compton, Berkshire, UK).

RP-HPLC(-MS) analysis and purification. Acetonitrile (ACN) and formic acid were purchased from VWR International (Darmstadt, Germany).

Gut-stability assays. Pancreatin from porcine pancreas (1x USP: product code (p.c.) ICNA0210255720, 102557, brand MP Biomedicals) was purchased from VWR International (Darmstadt, Germany) and from Sigma-Aldrich, Merck (Darmstadt, Germany) (4x USP: p.c. P1750). KH_2PO_4, NaOH pellets and HCl (6 M) were purchased from VWR International (Darmstadt, Germany). Double-distilled Milli-Q water (ddH_2O) was used for all buffer preparations.

Cell culture and in vitro pharmacology. HEK293 cells were purchased from American Type Culture Collection (ATCC, Manassas, VA, USA). Dulbecco's Modified Eagle's Medium (DMEM), Fetal Bovine Serum (FBS), L-glutamine and penicillin/streptomycin were purchased from Sigma-Aldrich, Merck (Darmstadt, Germany). G418 was purchased from Genaxxon Bioscience (Ulm, Germany). Inositol-1 phosphate (IP-1) assay kit as purchased from Cisbio (Codolet, France).

General peptide synthesis and purification.

Peptides were manually assembled on a 0.05 mmol scale using Fmoc-SPPS protocols as previously described.[90] Standard amino acid couplings were performed with 5 eq. excess of amino acid, 5 eq. HATU (0.5 M) and 6 eq. DIPEA in DMF (coupling time: 10 min). Fmoc was deprotected by treating the peptide-resin with 50% piperidine in DMF (1 min, twice). Unless otherwise stated, standard orthogonal protected Fmoc-amino acids were used as follows: Fmoc-Asn(Trt)-OH, Fmoc-Cys(Trt)-OH, Fmoc-Gln(Trt)-OH, Fmoc-Tyr(tBu)-OH. Upon complete assembly of the target sequences, dried peptide resins were treated with TFA:TIPS:ddH_2O = 90:5:5 (disulfide-cyclic analogues) or TFA:TIPS:DODT:DMS = 94:2:2:2 (thioether-cyclic analogues) to deprotect side-chains and cleave the peptides from the solid support (cleavage time: 90 min). TFA was removed under continuous nitrogen stream and crude peptides were precipitated by adding ice-cold Et_2O. Precipitates were

washed twice with fresh ice-cold Et_2O (resuspended and centrifuged), dissolved in 1:1 ddH_2O/ACN containing 0.1% TFA and freeze-dried. Linear sequences were cyclized using either cyclization method A (disulfide-cyclic analogues, in-solution), method B (thioether-cyclic analogues, on-resin) or method C (thioether cyclic analogous containing thioPro, on-resin). Specific synthesis and cyclization procedures are detailed individually below for each analogue class. Peptides were purified *via* preparative RP-HPLC on a Waters Auto Purification HPLC-UV system equipped with a Kromasil Classic C_4 column (21.2 × 250 mm, 300 Å, 10 µm) and UV detection at 214 nm. The following chromatographic parameters were used: flow rate of 20 mL/min and linear gradient elution of 5–45% solvent B in 40 min. Solvent A: 0.1% TFA in ddH_2O, solvent B: 0.08% TFA in ACN.

Peptide analysis and quality control *via* HPLC and (HR)-ESI-MS analysis and concentration determination for biological assays.

Routine reaction control and peptide analysis. Synthesis and cyclization reactions were monitored *via* RP-HPLC-UV-ESI-MS on a Thermo Scientific Dionex Ultimate 3000 system equipped with a UV-VIS detector (214 nm and 280 nm) and a Thermo Scientific MSQ Plus ESI-MS detector (positive ion mode). The following chromatographic parameters were used: linear-gradient elution (1–61% solvent B in 6 min) on a Waters Acquity UPLC BEH C_{18} column (2.1 × 50 mm,130 Å, 1.7 µm) with a flow rate of 1 mL/min at 30°C. Solvent A: 0.1% formic acid in ddH_2O, solvent B: 0.08% formic acid in ACN.

Final analysis – RP-HPLC. Chromatograms were recorded on a Thermo Scientific Vanquish Horizon UHPLC system with UV detection at 214 and 280 nm, using the following chromatographic parameters: linear-gradient elution (5–65% solvent B in 30 min) on a Kromasil Classic C_{18} column (4.6 × 150 mm, 300 Å, 5 µm) with a flow rate of 1 mL/min at 30°C. Solvent A: 0.1% TFA in ddH_2O, solvent B: 0.08% TFA in ACN. All synthesized final compounds were of >95% purity as determined by analytical RP-HPLC and relative peak quantification at 214 nm.

Final analysis - HR-MS. High-resolution mass spectra were recorded on a Thermo Scientific LTQ Orbitrap Velos mass spectrometer (positive ion mode, m/z range: 300-2000, FT resolution: 60,000). Samples were analyzed in LC-MS mode on a Vanquish Horizon UHPLC system using chromatographic parameters as follows: linear-gradient elution (10–65% solvent B in 14 min) on an Acclaim C_{18} HPLC column (2.1 x 150 mm, 120 Å, 3 µm, Thermo Fisher Scientific) with a flow rate of 0.45 mL/min at 30°C. Solvent A: 0.1% formic acid in ddH_2O, solvent B: 0.1% formic acid in ACN. The sum formulas of the detected ions were confirmed using Xcalibur 4.2.47 based on the mass accuracy ($\Delta m/z \leq 5$ ppm) and isotopic pattern.

Concertation determination for biological assays. The peptide content of each OT analogue was quantified against standards of known concentration (established *via* amino acid analysis) before use in any biological assay. In brief, stock solutions (3 mg/mL) in ddH_2O were prepared and samples of unknown concertation and three standards (OT and OT-like peptides of known concertation) were analyzed *via* HPLC-UV on a Kromasil Classic C_{18} column (2.1 × 100 mm, 100 Å, 5 µm) using UV detection at 214 nm. A 1 mL/min flow rate and linear gradient elution of 5-65% solvent B in 10 min at

30 °C were used. Solvent A: 0.1% TFA in ddH_2O, solvent B: 0.08% TFA in ACN. Peak areas of samples and standards (mean of three injections per peptide) were determined *via* manual integration, and peptide contents were calculated based on Lambert Beer's Law and calculated extinction coefficients.[90]

Peptide cyclization method A: disulfide-cyclic analogues. Linear sequences were manually assembled on a Fmoc-Rink amide AM resin (0.74 mm/g, swelled in DMF for 2 h) using the following cysteine side-chain protecting groups: Cys^1(Trt) (for OT analogues), Mpa^1(Trt) (for dOT analogues) and Cys^6(Trt). Linear peptides were cleaved from the solid support and isolated using standard conditions described under general peptide synthesis and purification. Crude linear precursor peptides were dissolved in aq. 0.1 M NH_4HCO_3 at pH 8.2 (peptide concentration: 200 µM) and stirred at air (25°C) until complete cyclization was indicated by analytical HPLC-MS analysis (overnight) (Figure S9). Folded products were isolated *via* preparative RP-HPLC using the general purification conditions.

Peptide cyclization Method B: thioether-cyclic analogues. Linear sequences were manually assembled on a low-loading TentaGel R RAM resin (Rink amide, 0.19 mmol/g), swelled in DCM for 1h and in DMF for 1 h. Upon incorporation of Fmoc-Cys^6(Mmt)-OH, the peptide-resin was treated with 1% TFA and 3% TIPS in DCM (5 min, 8 times) to remove the thiol side-chain protecting group. The resin was extensively washed with DMF and treated with allyl-4-bromobutanoate (10 eq., 1 M in DMF) and DIPEA (15 eq.) in a closed reaction vessel under argon atmosphere (1 h). The resin was extensively washed with DMF, and the remaining sequence was manually assembled using standard coupling conditions. Upon coupling of the last amino acid (position 2), the peptide resin was treated with $Pd(PPh_3)_4$ (1 eq., 0.05 M) and phenylsilane (50 eq.) in dry DCM in a closed reaction vessel under argon atmosphere (15 min, twice) to remove the allyl protecting group. The resin was washed with DCM and DMF, and Fmoc was removed with 50% piperidine in DMF (1 min, twice). The sequence was then cyclized on resin: PyBOP (2.5 eq., 0.5 M in DMF) and DIPEA (5 eq.) were added and incubated with the resin for 1 h (Figure S10). The cyclic products were cleaved from the solid support, isolated and purified using the standard conditions described in the general peptide synthesis and purification section.

Peptide cyclization Method C: thioether-cyclic analogues containing thioPro. Linear sequences were manually assembled on a low-loading TentaGel R RAM resin (Rink amide, 0.19 mmol/g), swelled in DCM for 1h and in DMF for 1 h. Cys was incorporated as Fmoc-Cys^6(Mmt)-OH and 4-bromobutyric acid (10 eq.) was coupled as the last residue using DIC (10 eq.)/Oxyma (10 eq., 0.5 M in DMF) mediated activation (1 h, twice). Upon assembly of the sequence, the resin was treated with 1% TFA and 3% TIPS in DCM (5 min, 8 times) to remove the thiol side-chain protecting group. The resin was extensively washed with DCM and DMF and treated with DIPEA (10 eq.) in DMF in a closed reaction vessel under argon atmosphere to initiate on-resin cyclization (overnight) (Figure S11). The

cyclic products were cleaved from the solid support, isolated and purified using standard conditions described in the general peptide synthesis and purification section.

Synthesis of allyl-4-bromobutanoat. A solution of allyl alcohol (1 eq.) and DIPEA (1.1 eq.) in dry chloroform (1 M) was stirred under ice-bath cooling in a Schlenk flask under argon atmosphere. 4-Bromobutyryl-chloride (1.1 eq.) was added dropwise over 15 min. The ice bath was removed and the mixture was let to 25 °C and stirred for 4 h (reaction control *via* TLC, EtOAc:heptane = 1:4). The solution was diluted with DCM and washed with aq. HCl (0.5 M, 3 times), aq. NaOH (0.5 M, 3 times) and brine, and dried over $MgSO_4$, and the solvent was then removed in vacuo The crude product was obtained as a yellowish oil and used without further purification.[129] The NMR spectra of allyl-4-bromobutanoat was recorded on a Bruker 400 MHz NMR device and was in accordance with the literature:[129] ^{1}H NMR (400 MHz, CDCl3) δ 5.95–5.84 (m, 1H), 5.30 (dd, J= 1.22, 17.21 Hz, 1H), 5.22 (dd, J=1.1, 10.42 Hz, 1H), 4.57 (d, J= 5.77 Hz, 2H), 3.45 (t, J=6.45 Hz, 2H), 2.53-2.50 (t, J= 7.18 Hz, 2H), 2.20-2.13 (m, 2H)

Synthesis of OT, dOT and analogue 4. Compounds were accessed using Cyclization Method A and general peptide synthesis and purification procedures. The following commercial non-standard amino acid building blocks were used: Mpa(Trt) (dOT), Fmoc-Lys(Ac)-OH (**4**).

Synthesis of analogues 1,2, 3, 6, 7, 8, and 9. Compounds were accessed using Cyclization Method A. Lys was incorporated as Fmoc-Lys^8(Mtt)-OH, Boc-Cys^1(Trt)-OH was coupled to the N-terminus of OT analogues (**1-3**) and Mpa^1(Trt) to the N-terminus of dOT analogues (**6-9**). All sequences were synthesized using standard conditions described in the general peptide synthesis and purification section. Upon assembly of the complete sequence, the peptide-resin was treated with 1% TFA and 3% TIPS in DCM (5 min, 8 times) to remove the Lys ε-amine side-chain protecting group followed by an extensive wash with DMF. The unprotected Lys^8 ε-amine side-chain was modified on-resin with various PEGylation motifs using Fmoc-NH-PEG_x-COOH (2.5 eq.), HATU (2.5 eq., 0.5 M) and DIPEA (5 eq.) in DMF overnight. The following commercial PEGylation building blocks were used: Fmoc-NH-PEG_3-COOH (**1, 2, 6, 8**) and Fmoc-NH-PEG_{27}-COOH (**3, 7, 9**). In the case of branched PEGylation motifs, Fmoc-Lys(Fmoc)-OH (**2, 8, 9**) was introduced as a branching element under standard coupling conditions, Fmoc protecting groups were removed with 50% piperidine in DMF (1 min, twice) and PEGylation was carried out as described above.

Synthesis of analogue 5. The compound was accessed using Cyclization Method A. Upon coupling of Fmoc-Dpr^8(Mtt)-OH, the peptide-resin was treated with 1% TFA and 3% TIPS in DCM (5 min, 8 times) to remove the β-amine side-chain protecting group followed by an extensive wash with DMF. The unprotected Dpr^8 β-amine side-chain was then acetylated by treating the peptide-resin with acetic anhydride (35 eq., 0.6 M) and DIPEA (55 eq.) in DMF (15 min, twice). The remaining sequence was synthesized using standard conditions described in the general peptide synthesis and purification section and conditions specified for cyclization method A. The following commercial non-standard amino acid building block was used: Fmoc-Dpr(Mtt)-OH.

Synthesis of carbetocin and analogues 10, 12, 15, 18, 20 and 22. Compounds were accessed using Cyclization Method B and general peptide synthesis and purification procedures. The following commercial non-standard amino acid building blocks were used: Fmoc-Lys(Ac)-OH, Fmoc-(C_α-Me)Leu-OH (**12**), Fmoc-Cpg-OH (**20, 22**), Fmoc-Tyr(Me)-OH (carbetocin, **10, 12, 22**), Fmoc-(C_α-Me)Tyr-OH (**15**) and Fmoc-(C_α-Me)Val-OH (**20**).

Synthesis of analogues 11, 13, 14, 16, 17, 19, and 21. Compounds were accessed using Cyclization Method B. Upon coupling of Fmoc-Dpr^8(Mtt)-OH, the peptide-resin was treated with 1% TFA and 3% TIPS in DCM (5 min, 8 times) to remove the β-amine side-chain protecting group followed by an extensive wash with DMF. The unprotected Dpr^8 β-amine side-chain was then acetylated by treating the peptide-resin with acetic anhydride (35 eq., 0.6 M) and DIPEA (55 eq) in DMF (15 min, twice). The remaining sequence was synthesized using standard conditions described under general peptide synthesis and purification and conditions specified for Cyclization Method B. The following commercial non-standard amino acid building blocks were used: Fmoc-Dpr(Mtt)-OH, Fmoc-(C_α-Me)Val-OH (**19**), Fmoc-Cpg-OH (**21**), Fmoc-Tyr(Me)-OH (**11**), Fmoc-Phe(4-Me)-OH (**13**), Fmoc-Phe(4-CF_3)-OH (**14**), Fmoc-(C_α-Me)Tyr-OH (**16**) and Fmoc-(C_α-Me)Phe-OH (**17**).

Synthesis of analogue 25. The compound was accessed using Cyclization Method B. Upon coupling of Fmoc-Dpr^8(Mtt)-OH, the peptide-resin was treated with 1% TFA and 3% TIPS in DCM (5 min, 8 times) to remove the β-amine side-chain protecting group followed by an extensive wash with DMF. The unprotected Dpr^8 β-amine side-chain was then acetylated by treating the peptide-resin with acetic anhydride (35 eq., 0.6 M) and DIPEA (55 eq.) in DMF (15 min, twice). The resin was extensively washed with DMF, and bromoacetic acid (10 eq.) was incorporated using DIC (10 eq.)/Oxyma (10 eq., 0.5 M in DMF) mediated activation (1 h). The resin was then reacted with 4-fluorobenzylamine (10 eq., 0.5 M) in DMF (1 h) to obtain the N-alkylated Gly^7 analogue.[108, 114] The remaining sequence was synthesized using standard conditions described in the general peptide synthesis and purification section and conditions specified for Cyclization Method B. The following commercial non-standard amino acid building blocks were used: Fmoc-Dpr(Mtt)-OH and Fmoc-Tyr(Me)-OH.

Synthesis of analogues 23, 24, 26, 27 and 28. Compounds were accessed using cyclization method C and general peptide synthesis and purification procedures. The following commercial non-standard amino acid building blocks were used: Fmoc-Lys(Ac)-OH, Fmoc-thioPro-OH, Fmoc-Cpg-OH (**23, 27**), Fmoc-Tyr(Me)-OH (**23, 24**), Fmoc-(C_α-Me)Tyr-OH (**26, 27**) and Fmoc-(C_α-Me)Val-OH (**28**).

Simulated intestinal fluid stability assays. SIF was prepared in accordance with USP specifications (USP 42 - NF 37, 2019) and peptide stabilities were tested following previously described protocols.[42, 91]

SIF preparation: KH_2PO_4 (68 mg, 6.8 mg/mL) was dissolved in 10 mL ddH_2O and the pH was adjusted to 6.8 using aq. 3 M NaOH. Pancreatin (100 mg, 1× USP for standard conditions, 4× USP for enhanced digestive strength) was added, the mixture was vortexed (1 min) and sonicated (15 min, 25°C). The fluid was centrifuged and syringe-filtered before use and prepared freshly daily.

Stability assay procedure: aq. TFA (5 vol%) was used as a stop-solution in all experiments to terminate digestion processes. At least three independent experiments (n ≥ 3) per compound were performed. The following sampling procedure describes a single independent experiment (n = 1): SIF (570 µL) was pre-incubated in a thermo shaker at 37 °C (15 min) before the test peptide stock solution (30 µL, 1 mM in ddH_2O) was added (50 µM final peptide concentration). The mixture was briefly vortexed, and t_0 samples (30 µL, duplicates) were drawn and added to an ice-cold stop solution (30 µL). Further samples (30 µL) were drawn at time points 2.5, 5, 15, 30, 60 min and at 2, 4, 6, 24 h for compounds with $t_{1/2}$ >60 min. For rapidly degrading compounds ($t_{1/2}$ <30 min), t_0 samples (duplicate) were prepared differently*:* SIF (28.5 µL) was quenched with stop solution (30 µL), vortexed, and the test peptide stock solution (1.5 µL) was added (duplicates). All samples were centrifuged (5 min, 16,000 × g) and stored at 4 °C before analysis*.*

RP-HPLC-UV(-MS) analysis: Stability samples were analyzed on a Dionex Ultimate 3000 system equipped with a UV-VIS detector (214 nm and 280 nm) and MSQ Plus ESI-MS detector (Thermo Scientific). Samples (30 µL) were injected onto a Waters Acquity UPLC BEH C_{18} column (2.1 × 50 mm,130 Å, 1.7 µm) and analyzed using the following chromatographic parameters: linear-gradient elution (5-65% solvent B in 6 min) and a flow rate of 1 mL/min at 30°C. Solvent A: 0.1% formic acid in ddH_2O. Solvent B: 0.08% formic acid in ACN. The mass identity of the compounds was confirmed via MS analysis (positive ion mode) over the time period of the assay.

Data analysis: Peak areas (mAU × min) at individual time points were determined by manual peak integration at 214 nm and normalized to time point zero (mean value of t_0 duplicate, $y(t_0)$ = 100%.). Half-lives ($t_{1/2}$) were calculated by fitting a one-phase exponential decay function to normalized data points via a nonlinear regression in GraphPad Prism (Version 9). Applied constraints: (i) $y(t_0)$ constant equal to 100, (ii) plateau constant equal to 0. Data were presented as mean ± standard error of the mean (SEM) of n ≥ 3 independent experiments. Please refer to the SI for full stability curves of all presented compounds.

***In vitro* pharmacology.**

Cell culture and stable cell line development: Cell lines stably expressing OTR and $V_{1a}R$ were prepared as previously described and used for all functional activity assays.[65, 130] In brief, HEK293 cells were transfected with pEGFP-N1-OTR and pEGFP-N1-$V_{1a}R$ plasmids[131] using jetPrime transfection reagent and standard protocols. Transfected cells were selected for plasmid incorporation by G418 antibiotic selection until a resistant population emerged and sorted *via* fluorescence-activated cell sorting (FACS) into 96-well plates to produce monoclonal cell populations. The highest receptor-expressing monoclonal cell population for each receptor was kept for further experiments. Stable HEK293-OTR and HEK293-$V_{1a}R$ cells were cultured and maintained in a humified 37°C incubator (with 5% CO_2) in Dulbecco's modified eagle medium (DMEM) supplemented with 10% FBS, 2 mM L-glutamine, 100 U/mL penicillin-streptomycin, and 200 µg/mL G418 antibiotic.

Inositol-1 phosphate (IP-1) accumulation assays were performed using the homogeneous time-resolved fluorescence (HTRF) IP-1 Gq kit (Cisbio) according to recommended protocols. Briefly, HEK293-OTR or HEK293-V_{1a}R cells were seeded into 384-well opaque white optiplates at a density of 10,000 cells/well. Following 48-hour maintenance, cell culture media was removed and replaced with 5 µL/well of stimulation buffer and the plate was kept in the incubator (37°C) for 15 min. Varying concentrations of peptides were then added to wells to stimulate receptors, and IP-1 was allowed to accumulate for 1 h at 37°C. IP-1 accumulation was stopped by addition of d2-IP-1 (in lysis and detection buffer) followed by terbium-cryptate labelled anti-IP-1 antibody (in lysis and detection buffer) and allowed to equilibrate with orbital shaking for 1 h at 25 °C. The HTRF signal (ratio of 665 nm / 620 nm emission) was measured in a TECAN Spark multimode plate reader. Data points for test peptides were normalised to the maximum and minimum of OT (for OTR) and VP (for V_{1a}R) and curves fitted by non-linear regression with a log(agonist) *vs* response (three parameters) equation in GraphPad Prism (Version 9).

Ca^{2+} mobilization assay: Initial OTR agonist activity screening (1st generation and some 2nd generation analogues) was done *via* Ca^{2+}-mobilization assay using a FLIPR^{TETR} platform and was generously provided by the National Institute of Mental Health's Psychoactive Drug Screening Program (NIMH PDSP).[132] For experimental details, please refer to the PDSP website (https://pdsp.unc.edu).

***In vivo* characterization.**

CVH model of chronic abdominal pain: Experiments were approved and performed in accordance with the guidelines of the Animal Ethics Committees of the South Australian Health and Medical Research Institute (SAHMRI) and Flinders University. Colitis was induced by the administration of dinitrobenzene sulfonic acid (DNBS) as described previously.[133, 134, 135, 136] Briefly, 13-week-old male mice (>25g) were fasted overnight with access to 5% glucose solution. After the fasting period, isofluorane-anaesthetised mice were administered an intracolonic enema of 0.1 mL DNBS (6.5 mg in 30% ethanol) via a polyethylene catheter inserted 3 cm past the anus. Mice were then individually housed with unlimited access to soaked food and 5% glucose solution and observed daily for changes in body weight, physical appearance, and behaviour. Histological examination of mucosal architecture, cellular infiltrate, crypt abscesses, and goblet cell depletion confirmed that DNBS induced significant damage by day 3 post-treatment, with mucosal architecture largely recovered by day 7, and fully recovered by 28 days post-treatment.[137] As high-threshold nociceptors from mice on day 28 post-treatment display significant mechanical hypersensitivity and lower mechanical activation thresholds. These mice also display hyperalgesia and allodynia and, therefore, termed chronic visceral hypersensitivity 'CVH mice'.[121, 133, 134, 135, 136, 138, 139]

Visceral Motor Response to Colorectal Distension: We recorded abdominal electromyographic (EMG) visceromotor responses (VMR) to colorectal distension (CRD) in fully awake animals.[121, 133, 134, 135, 136, 138, 139] Briefly, at least three days before assessment of VMR, under isoflurane anaesthesia, the bare endings of two Teflon-coated stainless-steel wires (Advent Research Materials Ltd, Oxford, UK) were

sutured into the right abdominal muscle. They were tunnelled subcutaneously and exteriorised at the base of the neck for future access. At the end of the surgery, mice received a prophylactic antibiotic (Baytril; 5 mg/kg s.c.) and an analgesic (buprenorphine; 0.4 mg/10 kg s.c.), then they were housed individually and allowed to recover. For intra-colonic delivery on the day of VMR recording, mice were briefly anaesthetised using isoflurane before receiving a 100 µL enema of vehicle (sterile saline). Then a lubricated balloon (2 cm in length) was gently introduced through the anus and inserted into the colorectum up to 0.25 cm past the anal verge. The balloon catheter was secured to the base of the tail and connected to a barostat (Isobar 3, G&J Electronics, Willowdale, Canada) for graded and pressure-controlled CRD. Mice were allowed to recover from anaesthesia in a restrainer with dorsal access for <15 min prior to initiation of the distension sequence. Distensions were applied at 20-40-50-60-70-80 mmHg (20 s duration each) at 2 min intervals so that the last distension was performed <30 min after intracolonic treatment. Immediately after VMR assessment, colonic compliance was assessed by applying graded volumes (40–200 µL, each of brief duration) to the balloon while recording the corresponding CRD pressures. Mice were returned to their cage, and later in the day, the procedure was repeated with mice briefly anaesthetised using isoflurane before receiving a 100 µL enema of analogue **26** (3.5 µg/kg equivalent to 1 µM or 350 µg/kg equivalent to 100 µM). Following the final distension, colonic compliance was re-assessed, and mice were subsequently humanely sacrificed by cervical dislocation. For oral dosing, CVH mice underwent baseline VMR to CRD testing and were then administered via oral gavage analogue **26** (2 mg/kg or 4 mg/kg) in a 100 µL bolus and VMR to CRDs re-assessed from 3.5–4 h post-administration. EMG electrodes were relayed to a data acquisition system, and the signal recorded (NL100AK headstage), amplified (NL104), filtered (NL 125/126, Neurolog, Digitimer Ltd, bandpass 50–5000 Hz) and digitised (CED 1401, Cambridge Electronic Design, Cambridge, UK) for off-line analysis using Spike2 (Cambridge Electronic Design). The analogue EMG signal was rectified and integrated. To quantify the magnitude of the VMR at each distension pressure, the area under the curve (AUC) during the distension (20 s) was corrected for baseline activity (AUC pre-distension, 20 s). We also calculated the total AUC, which is the summation of data points across all distension pressures for each individual animal or AUC to non-noxious (20-40 mmHg) or noxious (50-80 mmHg) distension pressures.

Statistical analysis: Data are presented as mean ± SEM, where N represents the number of animals. AUC data were statistically analysed to determine if they were normally distributed using a Shapiro-Wilk test. Based on these tests, data were then analysed with a paired t-test or Wilcoxon test. A *P* value <0.05 was considered statistically significant. Analysis and figures were prepared in GraphPad Prism (Version 9).

SUPPLEMENTARY INFORMATION.

Analytical characterization data (HPLC traces, mass spectra), complete SIF degradation curves, and pharmacological characterization data.

AUTHOR INFORMATION

Corresponding Author

*m.muttenthaler@uq.edu.au

ORCID

Thomas Kremsmayr: 0000-0003-0630-2555

Bradley L Hoare: 0000-0002-4011-7532

Stuart Brierley: 0000-0002-2527-2905

Markus Muttenthaler: 0000-0003-1996-4646

Author Contributions

T.K.: conceptualization (structure-activity relationship study and analogue design), investigation, formal analysis, methodology, visualization and writing – original draft. M.K.: investigation. B.H.: investigation. G.S: investigation, analysis, methodology. S.M.B: study design, analysis, funding acquisition, supervision, writing. M.M.: conceptualization, funding acquisition, supervision, and writing – review and editing. All authors have read, commented, and approved the final version of the manuscript.

Conflicts of Interest

The authors declare no competing financial interest. The University of Vienna has filed a patent application on oxytocin analogues described herein with T.K. and M.M. as inventors.

ACKNOWLEDGEMENTS

We thank Prof. Christian F.W. Becker (Institute of Biological Chemistry, University of Vienna) for his support of this work. We are grateful to the NIMH PDSP (National Institute of Mental Health's Psychoactive Drug Screening Program, Contract # HHSN-271-2018-00023-C), which is directed by Bryan L. Roth at the University of North Carolina at Chapel Hill and Project Officer Jamie Driscoll at NIMH, Bethesda MD, USA, for providing agonist functional activity data of OT variants (Ca^{2+} mobilization assay). We also thank Dr. Martin Zehl and the Mass Spectrometry Centre at the University of Vienna (a member of Vienna Life-Science Instruments) for assistance with HR-MS analysis. This research was supported by the European Research Council under the European Union's Horizon 2020 research and innovation program (grant agreement no. 714366), by the Australian Research Council (DP190101667, FT210100266) and by the Vienna Science and Technology Fund (WWTF, 10.47379/LS18053). T. Kremsmayr was supported by the Austrian Academy of Sciences through a DOC Fellowship (25139). S.M. Brierley was supported by a National Health and Medical Research Council of Australia (NHMRC) Investigator Leadership Grant (APP2008727).

ABBREVIATIONS

ACN, acetonitrile; Ac_2O, acetic anhydride; CRD, colorectal distension; CVH, chronic visceral hypersensitivity; 2-CTC, 2-chlorotrityl chloride; DIPEA, N,N-diisopropylethylamine; DNBS, dinitrobenzene sulfonic acid; DODT, 3,6-dioxa-1,8-octane-dithiol; EMG, electromyographic; Et_2O, diethyl ether; EtOAc, ethyl acetate; FDA, Food and Drug Administration; Fmoc-SPPS, 9-fluorenymethyloxycarbonyl-solid phase peptide synthesis; GC-C, guanylate cyclase-C; GPCR, G protein-coupled receptor; GdnHCl; guanidine hydrochloride; HATU, 1-[bis(dimethylamino)methylene]-1H-1,2,3-triazolo[4,5-b]pyridinium 3-oxide hexafluorophosphate; IBD, inflammatory bowel diseases; IBS, irritable bowel syndrome; IP-1; inositol 1-phosphate; OT, oxytocin; OTR, oxytocin receptor; ^{i}PrOH, 2-propanol; PyBOP, (benzotriazol-1-yloxy)tripyrrolidinophosphonium hexafluorophosphate; SGF, simulated gastric fluid; SIF, simulated intestinal fluid; TCEP, tris(2-carboxyethyl)phosphine; TIPS, triisopropylsilane; USP, U.S. Pharmacopeia; VMR, visceromotor response; VP, vasopressin; $V_{1a}R$, vasopressin 1a receptor

REFERENCES

1. Grundy L, Erickson A, Brierley SM. Visceral Pain. *Annual Review of Physiology* 2019, **81:** 261-284.

2. Camilleri M. Diagnosis and Treatment of Irritable Bowel Syndrome: A Review. *JAMA* 2021, **325**(9)**:** 865-877.

3. Enck P, Aziz Q, Barbara G, Farmer AD, Fukudo S, Mayer EA*, et al.* Irritable bowel syndrome. *Nature Reviews Disease Primers* 2016, **2:** 16014.

4. Bosman M, Weerts Z, Snijkers JTW, Vork L, Mujagic Z, Masclee AAM*, et al.* The Socioeconomic Impact of Irritable Bowel Syndrome: An Analysis of Direct and Indirect Health Care Costs. *Clin Gastroenterol Hepatol* 2023, **21**(10)**:** 2660-2669.

5. Roda G, Chien Ng S, Kotze PG, Argollo M, Panaccione R, Spinelli A*, et al.* Crohn's disease. *Nat Rev Dis Primers* 2020, **6**(1)**:** 22.

6. Kobayashi T, Siegmund B, Le Berre C, Wei SC, Ferrante M, Shen B*, et al.* Ulcerative colitis. *Nat Rev Dis Primers* 2020, **6**(1)**:** 74.

7. Kaplan GG, Windsor JW. The four epidemiological stages in the global evolution of inflammatory bowel disease. *Nat Rev Gastroenterol Hepatol* 2021, **18**(1)**:** 56-66.

8. Camilleri M. Management Options for Irritable Bowel Syndrome. *Mayo Clinic Proceedings* 2018, **93**(12)**:** 1858-1872.

9. Gros B, Kaplan GG. Ulcerative Colitis in Adults: A Review. *JAMA* 2023, **330**(10)**:** 951-965.

10. Szigethy E, Knisely M, Drossman D. Opioid misuse in gastroenterology and non-opioid management of abdominal pain. *Nature Reviews Gastroenterology & Hepatology* 2018, **15**(3)**:** 168-180.

11. Melchior C, Desprez C, Wuestenberghs F, Leroi AM, Lemaire A, Goucerol G. Impact of Opioid Consumption in Patients With Functional Gastrointestinal Disorders. *Frontiers in Pharmacology* 2020, **11:** 596467.

12. de Araujo AD, Mobli M, Castro J, Harrington AM, Vetter I, Dekan Z*, et al.* Selenoether oxytocin analogues have analgesic properties in a mouse model of chronic abdominal pain. *Nature Communications* 2014, **5:** 3165.

13. Gong L, Li J, Tang Y, Han T, Wei C, Yu X*, et al.* The antinociception of oxytocin on colonic hypersensitivity in rats was mediated by inhibition of mast cell degranulation via Ca^{2+}-NOS pathway. *Scientific Reports* 2016, **6:** 31452.

14. Perisic M, Woolcock K, Hering A, Mendel H, Muttenthaler M. Oxytocin and vasopressin signaling in health and disease. *Trends Biochem Sci* 2024, **49**(4)**:** 361-377.

15. Jurek B, Neumann ID. The Oxytocin Receptor: From Intracellular Signaling to Behavior. *Physiological Reviews* 2018, **98**(3)**:** 1805-1908.

16. Gimpl G, Fahrenholz F. The oxytocin receptor system: structure, function, and regulation. *Physiol Rev* 2001, **81**(2)**:** 629-683.

17. Welch MG, Tamir H, Gross KJ, Chen J, Anwar M, Gershon MD. Expression and developmental regulation of oxytocin (OT) and oxytocin receptors (OTR) in the enteric nervous system (ENS) and intestinal epithelium. *The Journal of Comparative Neurology* 2009, **512**(2)**:** 256-270.

18. Ohlsson B, Truedsson M, Djerf P, Sundler F. Oxytocin is expressed throughout the human gastrointestinal tract. *Regul Pept* 2006, **135**(1-2)**:** 7-11.

19. Monstein H-J, Grahn N, Truedsson M, Ohlsson B. Oxytocin and oxytocin-receptor mRNA expression in the human gastrointestinal tract: a polymerase chain reaction study. *Regulatory Peptides* 2004, **119**(1)**:** 39-44.

20. Kingsbury MA, Bilbo SD. The inflammatory event of birth: How oxytocin signaling may guide the development of the brain and gastrointestinal system. *Frontiers in Neuroendocrinology* 2019, **55:** 100794.

21. Ohlsson B, Ringström G, Abrahamsson H, Simrén M, Björnsson ES. Oxytocin stimulates colonic motor activity in healthy women. *Neurogastroenterology & Motility* 2004, **16**(2)**:** 233-240.

22. Qin J, Feng M, Wang C, Ye Y, Wang PS, Liu C. Oxytocin receptor expressed on the smooth muscle mediates the excitatory effect of oxytocin on gastric motility in rats. *Neurogastroenterology & Motility* 2009, **21**(4)**:** 430-438.

23. Yu Q, Ji R, Gao X, Fu J, Guo W, Song X*, et al.* Oxytocin is expressed by both intrinsic sensory and secretomotor neurons in the enteric nervous system of guinea pig. *Cell and Tissue Research* 2011, **344**(2)**:** 227-237.

24. Matsunaga M, Konagaya T, Nogimori T, Yoneda M, Kasugai K, Ohira H*, et al.* Inhibitory effect of oxytocin on accelerated colonic motility induced by water-avoidance stress in rats. *Neurogastroenterology & Motility* 2009, **21**(8)**:** 856-e859.

25. Tang Y, Shi Y, Gao Y, Xu X, Han T, Li J*, et al.* Oxytocin system alleviates intestinal inflammation by regulating macrophages polarization in experimental colitis. *Clinical Science* 2019, **133**(18)**:** 1977-1992.

26. Iseri SO, Sener G, Saglam B, Gedik N, Ercan F, Yegen BC. Oxytocin ameliorates oxidative colonic inflammation by a neutrophil-dependent mechanism. *Peptides* 2005, **26**(3)**:** 483-491.

27. Çetinel Ş, Hancıoğlu S, Şener E, Üner C, Kılıç M, Şener G*, et al.* Oxytocin treatment alleviates stress-aggravated colitis by a receptor-dependent mechanism. *Regulatory Peptides* 2010, **160**(1)**:** 146-152.

28. Shi Y, Li S, Zhang H, Zhu J, Che T, Yan B*, et al.* The effect of macrophage polarization on the expression of the oxytocin signalling system in enteric neurons. *Journal of Neuroinflammation* 2021, **18**(1)**:** 261.

29. Klein BY, Tamir H, Ludwig RJ, Glickstein SB, Welch MG, Anwar M. Colostrum oxytocin modulates cellular stress response, inflammation, and autophagy markers in newborn rat gut villi. *Biochemical and Biophysical Research Communications* 2017, **487**(1)**:** 47-53.

30. Gross Margolis K, Vittorio J, Talavera M, Gluck K, Li Z, Iuga A*, et al.* Enteric serotonin and oxytocin: endogenous regulation of severity in a murine model of necrotizing enterocolitis. *American Journal of Physiology - Gastrointestinal and Liver Physiology* 2017, **313**(5)**:** G386-G398.

31. Welch MG, Margolis KG, Li Z, Gershon MD. Oxytocin regulates gastrointestinal motility, inflammation, macromolecular permeability, and mucosal maintenance in mice. *American Journal of Physiology - Gastrointestinal and Liver Physiology* 2014, **307**(8)**:** G848-G862.

32. Chen D, Zhao J, Wang H, An N, Zhou Y, Fan J*, et al.* Oxytocin evokes a pulsatile PGE2 release from ileum mucosa and is required for repair of intestinal epithelium after injury. *Scientific Reports* 2015, **5:** 11731.

33. Alfvén G, Torre B, Uvnäs-Moberg K. Depressed concentrations of oxytocin and cortisol in children with recurrent abdominal pain of non-organic origin. *Acta Paediatrica* 1994, **83**(10)**:** 1076-1080.

34. Alfvén G. Plasma Oxytocin in Children with Recurrent Abdominal Pain. *Journal of Pediatric Gastroenterology and Nutrition* 2004, **38**(5)**:** 513-517.

35. Louvel D, Delvaux M, Felez A, Fioramonti J, Bueno L, Lazorthes Y*, et al.* Oxytocin increases thresholds of colonic visceral perception in patients with irritable bowel syndrome. *Gut* 1996, **39**(5)**:** 741-747.

36. Ohlsson B, Truedsson M, Bengtsson M, Torstenson R, Sjolund K, Bjornsson ES*, et al.* Effects of long-term treatment with oxytocin in chronic constipation; a double blind, placebo-controlled pilot trial. *Neurogastroenterology & Motility* 2005, **17**(5)**:** 697-704.

37. Wan J, Mobli M, Brust A, Muttenthaler M, Andersson A, Ragnarsson L*, et al.* Synthesis of Multivalent [Lys^8]-oxytocin Dendrimers that Inhibit Visceral Nociceptive Responses. *Australian Journal of Chemistry* 2017, **70**(2)**:** 162.

38. Li J, Xue B, Han T, Huang K, Gong L, Ma X*, et al.* Oxytocin down-regulates mesenteric afferent sensitivity via the enteric OTR/nNOS/NO/K_{ATP} pathway in rat. *Neurogastroenterology & Motility* 2015, **27**(1)**:** 51-62.

39. Xu S, Qin B, Shi A, Zhao J, Guo X, Dong L. Oxytocin inhibited stress induced visceral hypersensitivity, enteric glial cells activation, and release of proinflammatory cytokines in maternal separated rats. *European Journal of Pharmacology* 2018, **818:** 578-584.

40. Brierley SM, Linden DR. Neuroplasticity and dysfunction after gastrointestinal inflammation. *Nature Reviews Gastroenterology & Hepatology* 2014, **11**(10)**:** 611-627.

41. Drucker DJ. Advances in oral peptide therapeutics. *Nature Reviews Drug Discovery* 2019, **19**(4)**:** 277-289.

42. Kremsmayr T, Aljnabi A, Blanco-Canosa JB, Tran HNT, Emidio NB, Muttenthaler M. On the Utility of Chemical Strategies to Improve Peptide Gut Stability. *Journal of Medicinal Chemistry* 2022, **65**(8)**:** 6191–6206.

43. Fjellestad-Paulsen A, Söderberg-Ahlm C, Lundin S. Metabolism of vasopressin, oxytocin, and their analogues in the human gastrointestinal tract. *Peptides* 1995, **16**(6)**:** 1141-1147.

44. Wang J, Yadav V, Smart AL, Tajiri S, Basit AW. Toward oral delivery of biopharmaceuticals: an assessment of the gastrointestinal stability of 17 peptide drugs. *Molecular Pharmaceutics* 2015, **12**(3)**:** 966-973.

45. Walter R, Schwartz IL, Darnell JH, Urry DW. Relation of the Conformation of Oxytocin to the Biology of Neurohypophyseal Hormones. *Proceedings of the National Academy of Sciences of the United States of America* 1971, **68**(6)**:** 1355.

46. Koehbach J, Stockner T, Bergmayr C, Muttenthaler M, Gruber CW. Insights into the molecular evolution of oxytocin receptor ligand binding. *Biochemical Society Transactions* 2013, **41**(1)**:** 197-204.

47. du Vigneaud V, Ressler C, Swan CJM, Roberts CW, Katsoyannis PG, Gordon S. THE SYNTHESIS OF AN OCTAPEPTIDE AMIDE WITH THE HORMONAL ACTIVITY OF OXYTOCIN. *Journal of the American Chemical Society* 1953, **75**(19)**:** 4879-4880.

48. du Vigneaud V, Ressler C, Swan JM, Roberts CW, Katsoyannis PG. The Synthesis of Oxytocin. *Journal of the American Chemical Society* 1954, **76**(12)**:** 3115-3121.

49. Wisniewski K. Design of Oxytocin Analogs. In: Goetz G (ed). *Cyclic Peptide Design*. Humana, New York, NY, 2019, pp 235-271.

50. Manning M, Misicka A, Olma A, Bankowski K, Stoev S, Chini B*, et al.* Oxytocin and vasopressin agonists and antagonists as research tools and potential therapeutics. *Journal of Neuroendocrinology* 2012, **24**(4)**:** 609-628.

51. Hruby VJ, Smith CW. Chapter 4 - Structure-Activity Relationships of Neurohypophyseal Peptides. In: Smith CW (ed). *Chemistry, Biology, and Medicine of Neurohypophyseal Hormones and their Analogs*. Academic Press, 1987, pp 77-207.

52. Boissonnas RA, Guttmann S, Berde B, Konzett H. Relationships between the chemical structures and the biological properties of the posterior pituitary hormones and their synthetic analogues. *Experientia* 1961, **17**(9)**:** 377-390.

53. Schneider CH, Vigneaud Vd. Synthesis of D-Leucine-oxytocin, a Biologically Active Diastereoisomer of Oxytocin, and Demonstration of its Separability from Oxytocin upon Countercurrent Distribution. *Journal of the American Chemical Society* 1962, **84**(15)**:** 3005-3008.

54. Drabarek S, Vigneaud Vd. 2-D-Tyrosine-oxytocin and 2-D-Tyrosine-deamino-oxytocin, Diastereoisomers of Oxytocin and Deamino-oxytocin. *Journal of the American Chemical Society* 1965, **87**(17)**:** 3974-3978.

55. Ferraro JJ, du Vigneaud V. 7-D-Proline-oxytocin and Its Deamino Analog. Diastereoisomers of Oxytocin and Deamino-oxytocin. *Journal of the American Chemical Society* 1966, **88**(16)**:** 3847-3850.

56. Muttenthaler M, Andersson A, de Araujo AD, Dekan Z, Lewis RJ, Alewood PF. Modulating oxytocin activity and plasma stability by disulfide bond engineering. *Journal of Medicinal Chemistry* 2010, **53**(24)**:** 8585-8596.

57. Hope DB, Murti VVS, Vigneaud VD. Synthesis of 1-Hemi-D-cystine-oxytocin. *Journal of the American Chemical Society* 1963, **85**(22)**:** 3686-3688.

58. Manning M, du Vigneaud V. 6-Hemi-D-cystine-oxytocin, a Diastereoisomer of the Posterior Pituitary Hormone Oxytocin. *Journal of the American Chemical Society* 1965, **87**(17)**:** 3978-3982.

59. Dutta AS, Anand N, Kar K. Synthesis and Pharmacological Activity of 4-D-Glutamine-oxytocin, 5-D-Asparagine-oxytocin, and 4-D-Glutamine-5-D-asparagine-oxytocin. *Journal of Medicinal Chemistry* 1966, **9**(4)**:** 497-499.

60. Sciabola S, Goetz GH, Bai G, Rogers BN, Gray DL, Duplantier A*, et al.* Systematic N-methylation of oxytocin: Impact on pharmacology and intramolecular hydrogen bonding network. *Bioorganic & Medicinal Chemistry* 2016, **24**(16)**:** 3513-3520.

61. Ressler C. The Cyclic Disulfide Ring of Oxytocin. *Proceedings of the Society for Experimental Biology and Medicine* 1956, **92**(4)**:** 725-730.

62. Kablaoui N, Vanase-Frawley M, Sciabola S. Hybrid peptide-small molecule oxytocin analogs are potent and selective agonists of the oxytocin receptor. *Bioorganic & Medicinal Chemistry Letters* 2017.

63. Walter R, Havran RT, Schwartz IL. Synthetic metabolites of neurohypophyseal hormones. [Des-9-glycinamide]oxytocin and [des-9-glycinamide,des-8-leucine]oxytocin. *Journal of Medicinal Chemistry* 1976, **19**(2)**:** 328-330.

64. Zaoral M, Krchňák V. Cyclooxytocin, an oxytocin analogue with an enhanced stability of the secondary structure. *Collect Czech Chem Commun* 1977, **42**(12)**:** 3500-3509.

65. Dekan Z, Kremsmayr T, Keov P, Godin M, Teakle N, Dürrauer L*, et al.* Nature-inspired dimerization as a strategy to modulate neuropeptide pharmacology exemplified with vasopressin and oxytocin. *Chemical Science* 2021, **12**(11)**:** 4057-4062.

66. Smyth DG. Acetylation of Amino and Tyrosine Hydroxyl Groups: Preparation of inhibitors of oxytocin with no intrinsic activity on the isolated uterus. *Journal of Biological Chemistry* 1967, **242**(7)**:** 1592-1598.

67. Hruby VJ, Chow MS, Smith DD. Conformational and Structural Considerations in Oxytocin-Receptor Binding and Biological Activity. *Annual Review of Pharmacology and Toxicology* 1990, **30**(1)**:** 501-534.

68. Poláček I, Krejčí I, Nesvadba H, Rudinger J. Action of [1,6-Di-alanine]-oxytocin and [1,6-Di-serine]-oxytocin on the rat uterus and mammary gland in vitro. *European Journal of Pharmacology* 1970, **9**(2)**:** 239-245.

69. Claybaugh JR, Uyehara CFT. Metabolism of Neurohypophysial Hormones. *Annals of the New York Academy of Sciences* 1993, **689**(1)**:** 250-259.

70. Tuppy H. The Influence of Enzymes on Neurohypophysial Hormones and Similar Peptides. In: Berde B (ed). *Neurohypophysial Hormones and Similar Polypeptides*. Springer Berlin Heidelberg: Berlin, Heidelberg, 1968, pp 67-129.

71. Stymiest JL, Mitchell BF, Wong S, Vederas JC. Synthesis of Biologically Active Dicarba Analogues of the Peptide Hormone Oxytocin Using Ring-Closing Metathesis. *Organic Letters* 2003, **5**(1)**:** 47-49.

72. Smith CW, Walter R, Moore S, Makofske RC, Meienhofer J. Replacement of the disulfide bond in oxytocin by an amide group. Synthesis and some biological properties of [cyclo-(1-L-aspartic acid, 6-L-α,β-diaminopropionic acid)]oxytocin. *Journal of Medicinal Chemistry* 1978, **21**(1)**:** 117-120.

73. Zhao R, Shi P, Chen J, Sun S, Chen J, Cui J*, et al.* Chemical synthesis and biological activity of peptides incorporating an ether bridge as a surrogate for a disulfide bond. *Chemical Science* 2020, **11**(30)**:** 7927-7932.

74. Lebl M, Barth T, Jošt K. Synthesis, reduction, and pharmacological properties of the sulfoxides of some carba-analogues of oxytocin. *Collection of Czechoslovak Chemical Communications* 1978, **43**(6)**:** 1538-1556.

75. Beard R, Stucki A, Schmitt M, Py G, Grundschober C, Gee AD*, et al.* Building bridges for highly selective, potent and stable oxytocin and vasopressin analogs. *Bioorganic & Medicinal Chemistry* 2018, **26**(11)**:** 3039-3045.

76. Kourra C, Cramer N. Converting disulfide bridges in native peptides to stable methylene thioacetals. *Chemical Science* 2016, **7**(12)**:** 7007-7012.

77. Chini B, Manning M. Agonist selectivity in the oxytocin/vasopressin receptor family: new insights and challenges. *Biochem Soc Trans* 2007, **35**(4)**:** 737-741.

78. Muttenthaler M, Andersson A, Vetter I, Menon R, Busnelli M, Ragnarsson L*, et al.* Subtle modifications to oxytocin produce ligands that retain potency and improved selectivity across species. *Science Signaling* 2017, **10**(508)**:** eaan3398.

79. du Vigneaud V, Winestock G, Murti VVS, Hope DB, Kimbrough RD. Synthesis of 1-β-Mercaptopropionic Acid Oxytocin (Desamino-oxytocin), a Highly Potent Analogue of Oxytocin. *Journal of Biological Chemistry* 1960, **235**(12)**:** PC64-PC66.

80. Hope DB, Murti VVS, du Vigneaud V. A Highly Potent Analogue of Oxytocin, Desamino-oxytocin. *Journal of Biological Chemistry* 1962, **237**(5)**:** 1563-1566.

81. Poulsen EF. The Induction and Stimulation of Labour With Buccal Desaminooxytocin and Oxytocin Tablets. *Acta Obstetricia et Gynecologica Scandinavica* 1973, **52**(4)**:** 303-307.

82. Frič I, Kodíček M, Procházka Ž, Jošt K, Bláha K. Synthesis and circular dichroism of some analogues of deamino-1-carba-oxytocin with modifications of the amino-acid residue in position 2. *Collection of Czechoslovak Chemical Communications* 1974, **39**(5)**:** 1290-1302.

83. Rath W. Prevention of postpartum haemorrhage with the oxytocin analogue carbetocin. *Eur J Obstet Gynecol Reprod Biol* 2009, **147**(1)**:** 15-20.

84. Passoni I, Leonzino M, Gigliucci V, Chini B, Busnelli M. Carbetocin is a Functional Selective Gq Agonist That Does Not Promote Oxytocin Receptor Recycling After Inducing β-Arrestin-Independent Internalisation. *Journal of Neuroendocrinology* 2016, **28**(4).

85. Vilhardt H, Atke A, Barthova J, Ubik K, Barth T. Interaction of Chymotrypsin with Carbetocin ([1-deamino-1-monocarba-2-O-methyltyrosine]-oxytocin). *Pharmacology & Toxicology* 1997, **81**(3)**:** 147-150.

86. Golubow J, du Vigneaud V. Comparison of Susceptibility of Oxytocin and Desamino-Oxytocin to Inactivation by Leucine Aminopeptidase and α-Chymotrypsin. *Proceedings of the Society for Experimental Biology and Medicine* 1963, **112**(1)**:** 218-219.

87. Barth T. Chymotryptic cleavage of deamino analogues of oxytocin. *Collect Czech Chem Commun* 1977, **42**(1)**:** 195-200.

88. Barth T, Pliška V, Rychlík I. Chymotryptic and tryptic cleavage of oxytocin and vasopressin. *Collect Czech Chem Commun* 1967, **32**(3)**:** 1058-1063.

89. Hlaváček J, Frič I. The effect of non-coded amino acids on the degradation of oxytocin analogs with α-chymotrypsin. *Collect Czech Chem Commun* 1989, **54**(8)**:** 2261-2270.

90. Kremsmayr T, Muttenthaler M. Fmoc solid phase peptide synthesis of oxytocin and analogues. In: Werry EL, Reekie TA, Kassiou M (eds). *Oxytocin: Methods and Protocols*. Humana: New York, NY, 2022, pp 175-199.

91. United States Pharmacopeia and National Formulary. Rockville, Md.: The United States Pharmacopeial Convention; 2019.

92. Hicks C, Ramos L, Reekie T, Misagh GH, Narlawar R, Kassiou M*, et al.* Body temperature and cardiac changes induced by peripherally administered oxytocin, vasopressin and the non-peptide oxytocin receptor agonist WAY 267,464: a biotelemetry study in rats. *British Journal of Pharmacology* 2014, **171**(11)**:** 2868-2887.

93. Veronese FM, Pasut G. PEGylation, successful approach to drug delivery. *Drug Discovery Today* 2005, **10**(21)**:** 1451-1458.

94. Youn YS, Jung JY, Oh SH, Yoo SD, Lee KC. Improved intestinal delivery of salmon calcitonin by Lys^{18}-amine specific PEGylation: stability, permeability, pharmacokinetic behavior and in vivo hypocalcemic efficacy. *Journal of Controlled Release* 2006, **114**(3)**:** 334-342.

95. Modi ME, Majchrzak MJ, Fonseca KR, Doran A, Osgood S, Vanase-Frawley M*, et al.* Peripheral Administration of a Long-Acting Peptide Oxytocin Receptor Agonist Inhibits Fear-Induced Freezing. *Journal of Pharmacology and Experimental Therapeutics* 2016, **358**(2)**:** 164-172.

96. Snider B, Geiser A, Yu XP, Beebe EC, Willency JA, Qing K*, et al.* Long-Acting and Selective Oxytocin Peptide Analogs Show Antidiabetic and Antiobesity Effects in Male Mice. *Journal of the Endocrine Society* 2019, **3**(7)**:** 1423-1444.

97. Busnelli M, Kleinau G, Muttenthaler M, Stoev S, Manning M, Bibic L*, et al.* Design and Characterization of Superpotent Bivalent Ligands Targeting Oxytocin Receptor Dimers via a Channel-Like Structure. *Journal of Medicinal Chemistry* 2016, **59**(15)**:** 7152-7166.

98. Chini B, Chinol M, Cassoni P, Papi S, Reversi A, Areces L*, et al.* Improved radiotracing of oxytocin receptor-expressing tumours using the new [^{111}In]-DOTA-Lys^{8}-deamino-vasotocin analogue. *British Journal of Cancer* 2003, **89**(5)**:** 930-936.

99. Snell CR, Smyth DG. Biologically active macromolecular forms of oxytocin. [8-Lysine]oxytocin as a suitable ligand. *Biochemical Journal* 1977, **165**(1)**:** 43-47.

100. Pflimlin E, Zhou Z, Amso Z, Fu Q, Lee C, Muppiddi A*, et al.* Engineering a Potent, Long-Acting, and Periphery-Restricted Oxytocin Receptor Agonist with Anorexigenic and Body Weight Reducing Effects. *Journal of Medicinal Chemistry* 2020, **63**(1)**:** 382-390.

101. Kalaba P, Sanchez de la Rosa C, Möller A, Alewood PF, Muttenthaler M. Targeting the Oxytocin Receptor for Breast Cancer Management: A Niche for Peptide Tracers. *J Med Chem* 2024, **67**(3)**:** 1625-1640.

102. Meyerowitz JG, Robertson MJ, Barros-Alvarez X, Panova O, Nwokonko RM, Gao Y*, et al.* The oxytocin signaling complex reveals a molecular switch for cation dependence. *Nature Structural & Molecular Biology* 2022.

103. Kinoshita R, Kozaki I, Shimizu K, Shibata T, Ochiai A, Honda H. Agonist/Antagonist Activity of Oxytocin Variants Obtained from Free Cyclic Peptide Libraries Generated via Amino Acid Substitution. *ACS Omega* 2021.

104. Busby RW, Kessler MM, Bartolini WP, Bryant AP, Hannig G, Higgins CS*, et al.* Pharmacologic properties, metabolism, and disposition of linaclotide, a novel therapeutic peptide approved for the treatment of irritable bowel syndrome with constipation and chronic idiopathic constipation. *Journal of Pharmacology and Experimental Therapeutics* 2013, **344**(1)**:** 196-206.

105. Eisler K, Rudinger J, Šorm F. Analogues of oxytocin with isoleucine replaced by L-diethylalanine, L-cyclopentylglycine, and L- and D-cyclohexylglycine. *Collection of Czechoslovak Chemical Communications* 1966, **31**(12)**:** 4563−4580.

106. Wittelsberger A, Patiny L, Slaninova J, Barberis C, Mutter M. Introduction of a cis-Prolyl Mimic in Position 7 of the Peptide Hormone Oxytocin Does Not Result in Antagonistic Activity. *Journal of Medicinal Chemistry* 2005, **48**(21)**:** 6553-6562.

107. Rosamond JD, Ferger MF. Synthesis and some pharmacological properties of oxytocin analogues having L-thiazolidine-4-carboxylic acid in position 7. *Journal of Medicinal Chemistry* 1976, **19**(7)**:** 873-876.

108. Wisniewski K, Alagarsamy S, Galyean R, Tariga H, Thompson D, Ly B*, et al.* New, potent, and selective peptidic oxytocin receptor agonists. *Journal of Medicinal Chemistry* 2014, **57**(12)**:** 5306-5317.

109. Chen L, Ilham SJ, Feng B. Pharmacological Approach for Managing Pain in Irritable Bowel Syndrome: A Review Article. *Anesthesiology and Pain Medicine* 2017, **7**(2).

110. Erak M, Bellmann-Sickert K, Els-Heindl S, Beck-Sickinger AG. Peptide chemistry toolbox - Transforming natural peptides into peptide therapeutics. *Bioorganic & Medicinal Chemistry* 2018, **26**(10)**:** 2759-2765.

111. Muttenthaler M, King GF, Adams DJ, Alewood PF. Trends in peptide drug discovery. *Nature Reviews Drug Discovery* 2021, **20**(4)**:** 309-325.

112. Kong XD, Moriya J, Carle V, Pojer F, Abriata LA, Deyle K*, et al.* De novo development of proteolytically resistant therapeutic peptides for oral administration. *Nature Biomedical Engineering* 2020, **4**(5)**:** 560-571.

113. Postina R, Kojro E, Fahrenholz F. Separate agonist and peptide antagonist binding sites of the oxytocin receptor defined by their transfer into the V2 vasopressin receptor. *Journal of Biological Chemistry* 1996, **271**(49)**:** 31593-31601.

114. Ichinose W, Cherepanov SM, Shabalova AA, Yokoyama S, Yuhi T, Yamaguchi H*, et al.* Development of a Highly Potent Analogue and a Long-Acting Analogue of Oxytocin for the Treatment of Social Impairment-Like Behaviors. *Journal of Medicinal Chemistry* 2019, **62**(7)**:** 3297-3310.

115. Cherepanov SM, Miura R, Shabalova AA, Ichinose W, Yokoyama S, Fukuda H*, et al.* Synthesis of oxytocin derivatives lipidated via a carbonate or carbamate linkage as a long-acting therapeutic agent for social impairment-like behaviors. *Bioorganic & Medicinal Chemistry* 2019, **27**(15)**:** 3358-3363.

116. Barth T, Krejčí I, Kupková B, Jošt K. Pharmacology of cyclic analogues of deamino-oxytocin not containing a disulphide bond (carba analogues). *European Journal of Pharmacology* 1973, **24**(2)**:** 183-188.

117. Sadeghi M, Erickson A, Castro J, Deiteren A, Harrington AM, Grundy L*, et al.* Contribution of membrane receptor signalling to chronic visceral pain. *The International Journal of Biochemistry & Cell Biology* 2018, **98:** 10-23.

118. Bryant AP, Busby RW, Bartolini WP, Cordero EA, Hannig G, Kessler MM*, et al.* Linaclotide is a potent and selective guanylate cyclase C agonist that elicits pharmacological effects locally in the gastrointestinal tract. *Life Sciences* 2010, **86**(19-20)**:** 760-765.

119. Braga Emidio N, Tran HNT, Andersson A, Dawson PE, Albericio F, Vetter I*, et al.* Improving the gastrointestinal stability of linaclotide. *Journal of Medicinal Chemistry* 2021, **64**(12)**:** 8384-8390.

120. Brierley SM, Grundy L, Castro J, Harrington AM, Hannig G, Camilleri M. Guanylate cyclase-C agonists as peripherally acting treatments of chronic visceral pain. *Trends in Pharmacological Sciences* 2022, **43**(2)**:** 110-122.

121. Grundy L, Harrington AM, Castro J, Garcia-Caraballo S, Deiteren A, Maddern J*, et al.* Chronic linaclotide treatment reduces colitis-induced neuroplasticity and reverses persistent bladder dysfunction. *JCI Insight* 2018, **3**(19).

122. Castro J, Harrington AM, Hughes PA, Martin CM, Ge P, Shea CM*, et al.* Linaclotide inhibits colonic nociceptors and relieves abdominal pain via guanylate cyclase-C and extracellular cyclic guanosine 3',5'-monophosphate. *Gastroenterology* 2013, **145**(6)**:** 1334-1346.

123. Busby RW, Bryant AP, Bartolini WP, Cordero EA, Hannig G, Kessler MM*, et al.* Linaclotide, through activation of guanylate cyclase C, acts locally in the gastrointestinal tract to elicit enhanced intestinal secretion and transit. *European Journal of Pharmacology* 2010, **649**(1-3)**:** 328-335.

124. Moroz E, Matoori S, Leroux JC. Oral delivery of macromolecular drugs: Where we are after almost 100 years of attempts. *Advanced Drug Delivery Reviews* 2016, **101:** 108-121.

125. Werle M, Foger F. Peroral peptide delivery: Peptidase inhibition as a key concept for commercial drug products. *Bioorg Med Chem* 2018, **26**(10)**:** 2906-2913.

126. Anselmo AC, Gokarn Y, Mitragotri S. Non-invasive delivery strategies for biologics. *Nature Reviews Drug Discovery* 2019, **18**(1)**:** 19-40.

127. McConnell EL, Fadda HM, Basit AW. Gut instincts: explorations in intestinal physiology and drug delivery. *International Journal of Pharmaceutics* 2008, **364**(2)**:** 213-226.

128. Kararli TT. Comparison of the gastrointestinal anatomy, physiology, and biochemistry of humans and commonly used laboratory animals. *Biopharmaceutics & Drug Disposition* 1995, **16**(5)**:** 351-380.

129. Mart RJ, Liem KP, Wang X, Webb SJ. The Effect of Receptor Clustering on Vesicle−Vesicle Adhesion. *Journal of the American Chemical Society* 2006, **128**(45)**:** 14462-14463.

130. Hicks C, Jorgensen W, Brown C, Fardell J, Koehbach J, Gruber CW*, et al.* The nonpeptide oxytocin receptor agonist WAY 267,464: receptor-binding profile, prosocial effects and distribution of c-Fos expression in adolescent rats. *J Neuroendocrinol* 2012, **24**(7)**:** 1012-1029.

131. Koehbach J, O'Brien M, Muttenthaler M, Miazzo M, Akcan M, Elliott AG*, et al.* Oxytocic plant cyclotides as templates for peptide G protein-coupled receptor ligand design. *Proceedings of the National Academy of Sciences of the United States of America* 2013, **110**(52)**:** 21183-21188.

132. Kroeze WK, Sassano MF, Huang XP, Lansu K, McCorvy JD, Giguere PM*, et al.* PRESTO-Tango as an open-source resource for interrogation of the druggable human GPCRome. *Nature Structural & Molecular Biology* 2015, **22**(5)**:** 362-369.

133. Jiang Y, Castro J, Blomster LV, Agwa AJ, Maddern J, Schober G*, et al.* Pharmacological Inhibition of the Voltage-Gated Sodium Channel NaV1.7 Alleviates Chronic Visceral Pain in a Rodent Model of Irritable Bowel Syndrome. *ACS Pharmacology & Translational Science* 2021, **4**(4)**:** 1362-1378.

134. Muratspahic E, Tomasevic N, Koehbach J, Duerrauer L, Hadzic S, Castro J*, et al.* Design of a Stable Cyclic Peptide Analgesic Derived from Sunflower Seeds that Targets the kappa-Opioid Receptor for the Treatment of Chronic Abdominal Pain. *J Med Chem* 2021, **64**(13)**:** 9042-9055.

135. Castro J, Garcia-Caraballo S, Maddern J, Schober G, Lumsden A, Harrington A*, et al.* Olorinab (APD371), a peripherally acting, highly selective, full agonist of the cannabinoid receptor 2, reduces colitis-induced acute and chronic visceral hypersensitivity in rodents. *Pain* 2022, **163**(1)**:** e72-e86.

136. Castro J, Harrington AM, Lieu T, Garcia-Caraballo S, Maddern J, Schober G*, et al.* Activation of pruritogenic TGR5, MrgprA3, and MrgprC11 on colon-innervating afferents induces visceral hypersensitivity. *JCI Insight* 2019, **4**(20).

137. Hughes PA, Brierley SM, Martin CM, Brookes SJH, Linden DR, Blackshaw LA. Post-inflammatory colonic afferent sensitisation: different subtypes, different pathways and different time courses. *Gut* 2009, **58**(10)**:** 1333-1341.

138. Salvatierra J, Castro J, Erickson A, Li Q, Braz J, Gilchrist J*, et al.* NaV1.1 inhibition can reduce visceral hypersensitivity. *JCI Insight* 2018, **3**(11).

139. Castro J, Grundy L, Deiteren A, Harrington AM, O'Donnell T, Maddern J*, et al.* Cyclic analogues of alpha-conotoxin Vc1.1 inhibit colonic nociceptors and provide analgesia in a

mouse model of chronic abdominal pain. *British Journal of Pharmacology* 2018, **175**(12)**:** 2384-2398.